MAPK, with RANK (22–24). Recently, SHP-1 was reported to interact with TRAF6 (25). Although lipopolysaccharide (LPS) is known to accelerate the bone lysis (26, 27) and promote the survival of osteoclasts (28), signaling via TLRs has never been reported to induce mature osteoclasts without RANKL (4). We reported that *in vivo* LPS injection increased the generation of BM osteoclast precursors, but the maturation from even these treated cells into $TRAP^+$cells required RANKL and M-CSF (29). Moreover, a cloned macrophage-like cell that lacks the *p53* gene differentiates into mature osteoclasts without M-CSF; however, RANKL is essential for its maturation (29–31). Therefore, signaling via TLRs may be insufficient as a substitute for RANK signaling.

In this study we showed that SHP-1 deficiency enabled BM cells treated with LPS plus M-CSF in the absence of RANKL to give rise to mature osteoclasts that resorb bone. The osteoclastogenesis does not depend on the production of RANKL or TNFα. These results indicate that SHP-1 regulates downstream signaling for osteoclastogenesis through not only receptor tyrosine kinases, but also members of the TNF receptor superfamily.

Materials and Methods

Mice

C57BL/6 (B6) mice were purchased from Japan-Clea (Yokohama, Japan). C57BL/6J-*Hcph*$^{me\text{-}v}$/*Hcph*$^{me\text{-}v}$ homozygotes (*me*^{v}/*me*^{v}) and their littermates (+/?) were raised at The Jackson Laboratory (Bar Harbor, ME). All mice were used at 7–16 wk of age.

Cell preparation and cultures

Mice were killed by cervical dislocation under ether anesthesia. BM cells were collected by flushing femoral shafts using a 26-gauge sterile needle. Cells from the peritoneal cavity (PECs) were obtained by injecting 4–8 ml ice-cold αMEM (Life Technologies, Inc., Grand Island, NY) supplemented with 10% fetal bovine serum (FBS; BioWhittaker, Walkersville, MD), 50 U/ml streptomycin, and 50 μg/ml penicillin (Meiji Chemical Co. Ltd., Tokyo, Japan).

To induce osteoclast differentiation, BM cells (1–2 $\times$ 10^4/well) and PECs (2–10 $\times$ 10^4/well) were cultured in 24-well plates (Corning Costar, Corning, NY) with 1 ml αMEM-supplemented 10% FBS and antibiotics in the presence of 50 ng/ml human M-CSF (a gift from Otsuka Pharmaceutical Co. Ltd., Tokushima, Japan) and/or 25 or 50 ng/ml recombinant human soluble RANKL (PeproTech EC Ltd., London, UK), 50 ng/ml recombinant mouse TNFα (R&D Systems, Inc., Place, NE), or TLR ligands for 6 d. According to the manufacturer, RANKL was produced by *Escherichia coli*, but the endotoxin level in the RANKL is less than 0.1 ng/μg. Cultures were fed every 3 d by replacing spent medium with fresh medium.

The number of multinucleated $TRAP^+$cells ($TRAP^+$ MNCs) was expressed as the mean ± SD of triplicate cultures (32). In some experiments, 20 ng/ml recombinant human IL-1α (a gift from Dr. S. Ono, Osaka University, Osaka, Japan) and 400 ng/ml human osteoprotegerin (OPG), a decoy receptor for RANKL (PeproTech EC Ltd.) were added to the cultures.

Pit formation assay

BM cells (5 $\times$ 10^3/well) were cultured on dentine slices (a gift from Dr. N. Udagawa, Matsumoto Dental University, Nagano, Japan) in 0.2 ml αMEM containing 10% FBS and 50 ng/ml M-CSF with 50 ng/ml soluble RANKL or 50 ng/ml LPS for 20 d in 96-well plates. After removal of the cells with 2 N NaOH, the slices were stained with 2% Coomassie Brilliant Blue R250 in methanol to visualize resorption pits (14).

TLR ligands

LPS from *Salmonella minnesota Re 595* (Sigma-Aldrich Corp., St. Louis, MO) or *E. coli 055 B5* (Difco, Detroit, MI) were used for *in vitro* and *in vivo* experiments. As both LPS preparations induce similar responses, most experiments used *S. minnesota R595* LPS unless otherwise indicated. Peptidoglycan (PGN) from *Staphylococcus aureus* (Fluka Chemie, Buchs, Switzerland), used to stimulate TLR2, was dissolved in water, sonicated, and sterilized in a hot water bath. A phosphorothioated oligonucleotide (ODN; 5′-TCC ATG ACG TTC CTG ATG CT-3′; CpG), used as an unmethylated CpG ODN to stimulate TLR9, and a control phosphorothioated ODN (5′-GCT TGA TGA CTC AGC CGG AA-3′) were purchased from Hokkaido System Science (Hokkaido, Japan) (33).

Antibodies (Abs)

An antagonistic rat antimouse TNFα monoclonal Ab (XT3) was purchased from Endogen (Woburn, MA) and used at 5 μg/ml for inhibition of TNFα activity. A nonantagonistic rat antimouse Kit Ab (ACK4) (34) was used as a control.

For flow cytometric analysis, monoclonal Abs against Fms (AFS98, biotinylated) (35), Kit [ACK2, phycoerythrin (PE)-conjugated[(34), or Mac-1 (CD11b, FITC-conjugated; M1/70, BD PharMingen, San Diego, CA) were used in Hanks' medium containing 2% BSA (fraction V, Sigma-Aldrich Corp.) and 0.05% NaN_3. The stained cells were analyzed using an EPICS-XL flow cytometer (Coulter Electronics, Hialeah, FL). Magnetic cell sorting for Kit-positive cell separation from BM cells was performed using the Mini-MACS column with PE-conjugated ACK2 and anti-PE antibody-conjugated microbeads (Miltenyi Biotec, Bergisch Gladbach, Germany).

RT-PCR

To determine the expression of TNFα (encoded by *Tnf*), RANKL (*Tnfsf11*), IL-1 receptor-associated kinase (IRAK) (*Irak1*), IRAK-M (*Irak3*), and hypoxanthine phosphoribosyl transferase (*Hprt*) genes, RT-PCR was performed. Total RNA was isolated using Isogen (Nippon Gene, Toyama, Japan) and was reverse transcribed using Reverse TraAce (Toyobo, Osaka, Japan). The DNA fragments were amplified from the mouse cDNAs by PCR. Hot-lid PCR amplification of cDNA equivalent to 20, 2, and 0.2 ng total RNA was carried out in 1× PCR buffer (1.5 mM $MgCl_2$) containing 0.2 mM deoxy-NTPs (Takara, Shiga, Japan), 0.75 U r*Taq* DNA polymerase (Toyobo), and primers (used at 1.2 μM). Amplifications were carried out on DNA thermal cyclers (MJ Research, Inc., Watertown, MA). After an initial 3-min denaturing step (94 C), each PCR cycle consisted of 45-sec denaturing (94 C), 1-min annealing (55 or 60 C), and 1.5-min elongation (72 C). After the final cycle, the reaction was held for 3 min at 72 C. The PCR products were then separated on a 2% agarose gel, stained with ethidium bromide, and photographed. The primers used here were as follows: *Tnf*, 5′-CAC GCT CTT CTG TCT ACT GAA CTT CG-3′ and 5′-GGC TGG GTA GAG AAT GGA TGA ACA CC-3′; *Tnfsf11*, 5′-CAG CAC TCA CTG CTT TTA TAG AAT CC-3′ and 5′-AGC TGA AGA TAG TCT GTA GGT ACG C-3′; *Irak1*, 5′-GCC AGT GGA AAG TGA TGA GAG TG-3′ and 5′-GAA AAA GCC TGA TGA CAG CAG TTG-3′; *Irak3*, 5′-TCC TTC AGG TGT CCT TCT CCA CTG-3′ and 5′-CCT CTT CTC CAT TGG CTT GCT C-3′; and *Hprt*, 5′-AAT GAT CAG TCA ACG GGG GAC A-3′ and 5′-CCA GCA AGC TTG CA ACCT TAA CCA-3′.

MAPK inhibitors

Inhibitors of the MAPK signaling pathway, PD098059 (2′-amino-3′ methoxyflavone; Wako Pure Industry, Kyoto, Japan) for MAPK kinase (ERK1/2), SB203580 [4-(4-fluorophenyl)-2-(4-methylsulfinylphenyl)-5-(4-pyridyl)1H-imidazole; Wako] for p38, and SP600125 [anthrax(1-9-cd)pyrazol-6(2H)-one; Tocris Cookson Ltd., Avonmouth, UK] for c-Jun N-terminal kinase, were dissolved to 20 mM in dimethylsulfoxide and used at 20 μM.

Statistical analysis

Data are presented as the mean ± SD. Statistical significance was assessed by *t* test.

Results

LPS induces osteoclastogenesis from me^v/me^v BM cells

To induce osteoclastogenesis, BM cells from SHP-1-deficient me^v/me^v mice and their wild-type littermates (+/?) were cultured with M-CSF and RANKL for 6 d. me^v/me^v BM cells developed 1.5–4 times higher numbers of multinucleated TRAP$^+$ cells (TRAP$^+$ MNCs) than their +/? littermates (Fig. 1A, *left*) (12, 13). The TLR family shares some of the downstream signaling via RANK (22–24). However, signaling via TLRs has never been reported to induce osteoclastogenesis without RANKL-RANK signaling (4). We cultured BM cells from me^v/me^v and +/? littermates with LPS plus M-CSF for 6 d. Although TRAP$^+$ mononuclear cells were generated, few TRAP$^+$ MNCs were detected in the wild-type littermate cultures even in the presence of up to 200 ng/ml LPS (Fig. 1A, *right*, and Fig. 1B). In the presence of LPS and M-CSF, me^v/me^v BM cells gave rise to significantly higher numbers of TRAP$^+$ mononuclear cells and TRAP$^+$ MNCs than normal littermates (Fig. 1C). The number of TRAP$^+$ MNCs induced by LPS (20 ng/ml) and M-CSF was 1/10th to 1/3rd of those induced with RANKL (50 ng/ml) and M-CSF in me^v/me^v BM cultures (Fig. 1A, *right*). Osteoclastogenesis was increased in a dose-dependent manner for the LPS added (Fig. 1B). Osteoclasts from me^v/me^v BM cells induced by M-CSF and LPS had bone-resorbing activity on dentine slices, although the activity of pit formation was lower than that induced by M-CSF and RANKL (Fig. 1D).

One receptor for LPS activation is known to be a TLR4, a member of the TLR superfamily (36). To assess whether the inductive effect on osteoclastogenesis is specific for LPS-TLR4 signaling or is a general characteristic of signaling via TLR superfamily members, we examined the effects of ligands for other TLRs, PGN for TLR2 (37) and unmethylated CpG for TLR9 (33), on osteoclastogenesis in the presence of M-CSF. PGN or CpG showed little inductive effect on osteoclastogenesis in either me^v/me^v or +/? mice (Fig. 2A, *left*). As recently reported, CpG inhibited osteoclast development of BM cells from both me^v/me^v and +/? control mice induced by RANKL and M-CSF (Fig. 2A, *right*) (29, 38). This indicates that LPS, but not other TLR ligands tested here, induces osteoclastogenesis of SHP-1-deficient BM cells in the presence of M-CSF.

We also compared the effects of inhibitors of MAPK sig-

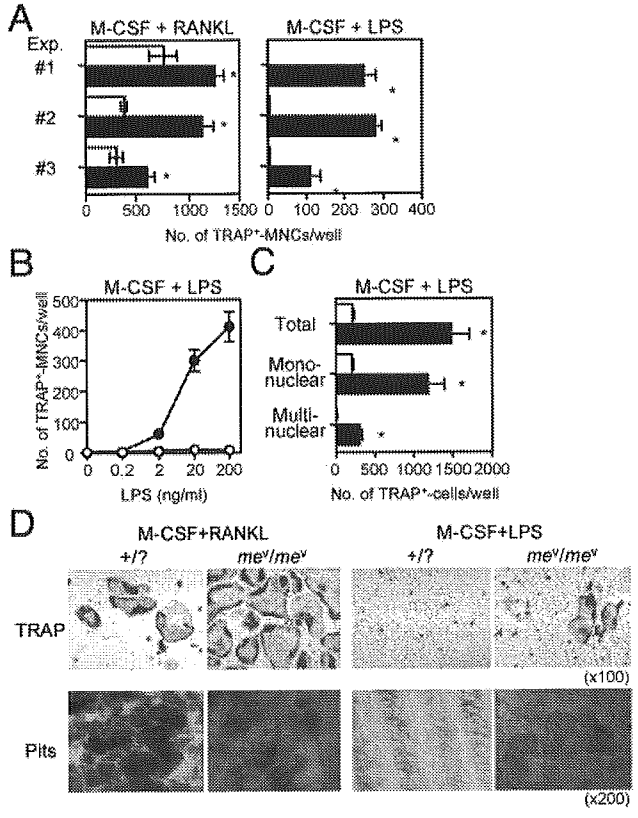

FIG. 1. Osteoclastogenesis of me^v/me^v BM cells induced by M-CSF and LPS. BM cells from me^v/me^v mice (■) and their wild-type littermates (+/?; □) were cultured with RANKL (A, *left*) or LPS in the presence of M-CSF for 6 d. LPS was added at 20 ng/ml (A, *right*; C and D), and varying doses (B; 0–200 ng/ml). A, Numbers of TRAP$^+$ MNCs from three representative experiments. C, Numbers of total, mononuclear, and multinuclear TRAP$^+$ cells. D, Photomicrographs of TRAP-stained cultures (d 6; magnification, ×100) and pit formation on dentine slices (d 20; magnification, ×200) of +/? (*left*) and me^v/me^v (*right*) BM cells. Significant differences compared with the responses of +/? littermates are indicated by an *asterisk* ($P < 0.05$). In all experiments, no TRAP$^+$cells were observed without M-CSF.

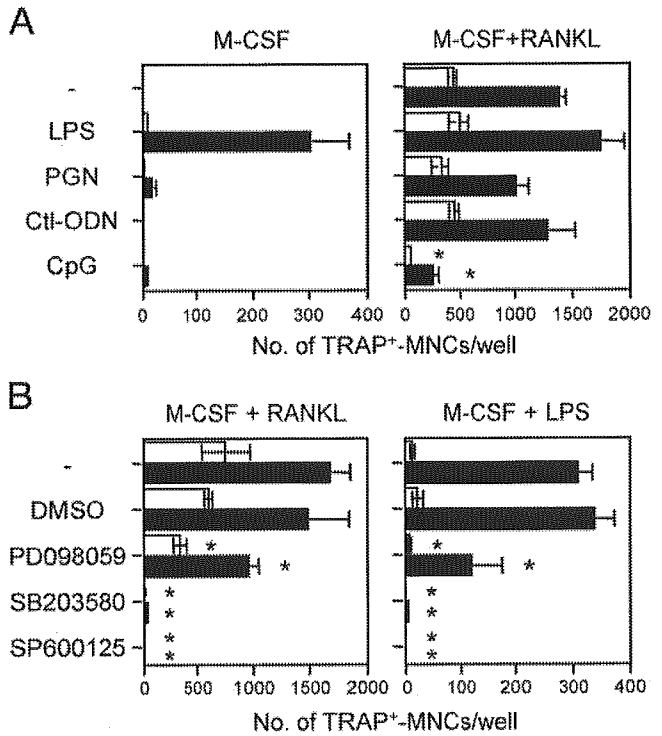

FIG. 2. LPS induces osteoclastogenesis from me^v/me^v BM cells. A, BM cells (2×10^4) from me^v/me^v mice (■) and their wild-type littermates (□) were cultured with or without 20 ng/ml LPS, 1 μg/ml PGN, 0.1 μM control ODN, or 0.1 μM CpG-ODN in the presence of 50 ng/ml M-CSF (*left*) or M-CSF plus RANKL (*right*) for 6 d. B, BM cells cultured with or without 20 μM MAPK inhibitors or the vehicle control dimethylsulfoxide (0.1%, vol/vol) in the presence of M-CSF and RANKL (*left*) or M-CSF and LPS (*right*) for 6 d. Significant differences compared with the responses of untreated cultures are indicated by an *asterisk* ($P < 0.05$). In all experiments, no TRAP$^+$ cells were observed without M-CSF.

naling on RANKL- and LPS-induced osteoclastogenesis. Inhibitors (20 μM) of the MAPK signaling pathway, PD098059 for MEK (ERK1/2), SB203580 for p38, and SP600125 for c-Jun N-terminal kinase, were added to the cultures for 6 d (Fig. 2B). SB203580 and SP600125 completely inhibited osteoclastogenesis in BM cells cultured with RANKL plus M-CSF and with LPS plus M-CSF. Although PD098059 did not completely inhibit osteoclastogenesis in either culture condition, this MAPK inhibitor reduced levels of osteoclastogenesis equivalently in these two culture system.

LPS-induced osteoclast development of me^v/me^v BM cells is not accounted for by the production of RANKL or TNFα

A recent report showed that TNFα mimicked the function of RANKL for stimulating *in vitro* osteoclastogenesis of BM cells (21). BM cells from me^v/me^v and +/? mice were cultured with 50 ng/ml TNFα or 50 ng/ml RANKL in the presence of M-CSF for 6 d, and comparable numbers of osteoclasts in the cultures with TNFα or RANKL were observed in the BM cell cultures from each mouse stain (Fig. 3A). We also incubated the cultures with M-CSF and IL-1α, but osteoclasts were not generated from either me^v/me^v or their littermate BM cells (Fig. 3A).

As LPS is known to induce TNFα production (28), we examined whether LPS-induced osteoclastogenesis was related to TNFα or RANKL production. If BM cells of me^v/me^v mice may produce high levels of TNFα or RANKL, osteoclastogenesis should occur in me^v/me^v BM cells. Therefore, BM cells from me^v/me^v and +/? mice were cultured with M-CSF, or M-CSF plus LPS for 3 d. Although LPS addition increased the expression of the TNFα (*Tnf*) gene transcript and induced a small amount of transcript of the RANKL (*Tnfsf11*) gene, doses of transcripts of *Tnf* and *Tnfsf11* genes were comparable in both strains of mice (Fig. 3B).

Recently, Kobayashi *et al.* (36–39) reported that IRAK (encoded by *Irak1*) associated with MyD88 and IRAK-M (encoded by *Irak3*) regulate the signaling via TLRs. We assessed the expression of *Irak1* and *Irak3* in BM cells cultured with M-CSF or M-CSF plus LPS. *Irak3* gene expression was increased in the presence of LPS as reported; however, no significant difference was detected between me^v/me^v and +/? cultured cells (Fig. 3B). An alternative possibility was that me^v/me^v BM cells may require a smaller amount of TNFα or RANKL to induce osteoclast development than wild-type BM cells, and LPS induces sufficient production of TNFα or RANKL to support osteoclastogenesis only in me^v/me^v BM cells. Thus, minimal requirements of TNFα or RANKL to induce $TRAP^+$ MNCs in cultures were assessed. More than 1 ng/ml TNFα or RANKL (Fig. 3C) was needed to induce osteoclastogenesis from both me^v/me^v and wild-type littermate BM cells.

To further confirm these observations, me^v/me^v BM cells were cultured with anti-TNFα antagonistic antibody (XT3) or OPG in the presence of M-CSF and LPS, and the inhibitory effect on LPS-induced osteoclastogenesis in me^v/me^v BM cells was observed. OPG and XT3 completely inhibited M-CSF and RANKL (50 ng/ml)-induced and M-CSF and TNFα (50 ng/ml)-induced osteoclastogenesis, respectively; however, neither reagent inhibited M-CSF plus LPS-induced osteoclastogenesis (Fig. 4). Although less than 1 ng/ml RANKL or TNFα might be produced by BM cells in the cultures, these results suggest that SHP-1 regulates the magnitude of osteoclastogenesis, but not the minimal requirements of RANKL or TNFα, and indicate that osteoclast development by me^v/me^v BM cells induced by M-CSF plus LPS may not be directly related to the production of RANKL or TNFα.

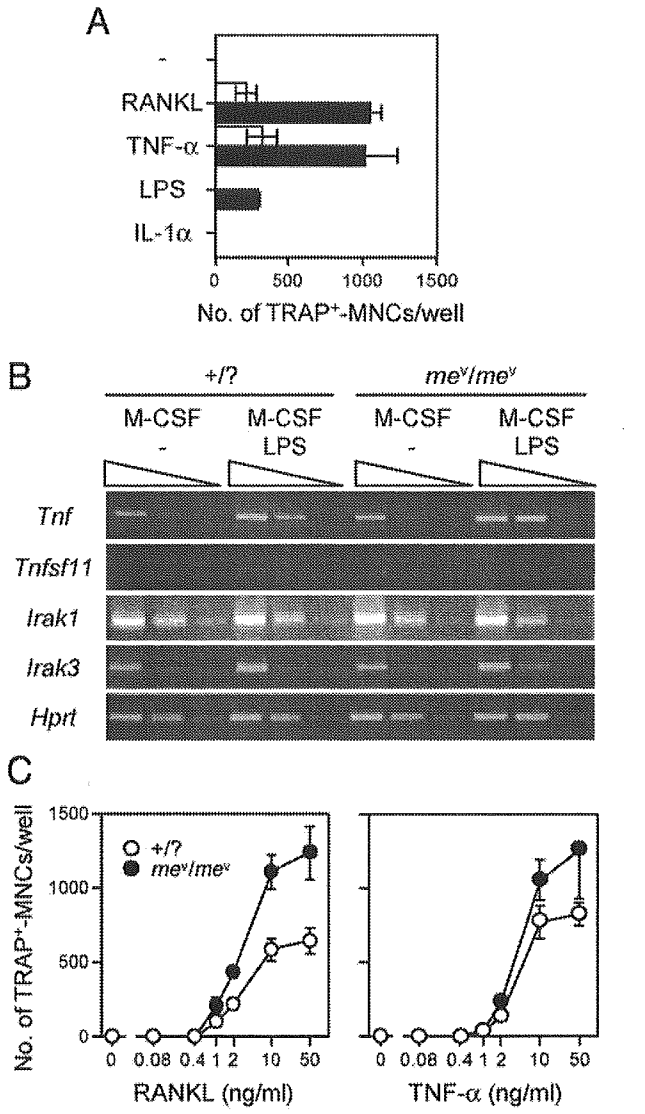

FIG. 3. Effects of LPS, TNFα, and IL-1α on osteoclastogenesis. A, BM cells (2×10^4) from +/? littermates (□) or me^v/me^v mice (■) were cultured with M-CSF and RANKL, 20 ng/ml LPS, TNFα, or IL-1α for 6 d. The mean number and SD of $TRAP^+$ MNCs per well from the simultaneous experiments are shown. B, cDNA from BM cells of +/? littermates and me^v/me^v mice cultured with M-CSF or M-CSF plus LPS for 3 d were prepared, and RT-PCRs for *Tnf*, *Tnfsf11*, *Irak1*, and *Irak4* were performed. Sequential doses of cDNA (equivalent to 20, 2, and 0.2 ng total RNA) were used as a template. Control responses were indicated by using primers for *Hprt*. C, Osteoclastogenesis induced by serial doses of RANKL (*left*) or TNFα (*right*) in the presence of M-CSF. In all experiments, no $TRAP^+$ cells were observed without M-CSF.

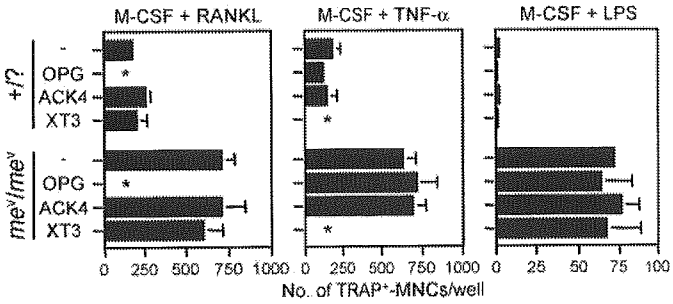

FIG. 4. LPS-induced osteoclastogenesis is not inhibited by OPG or anti-TNFα antibody. BM cells (2×10^4) from +/? littermates (*top*) or me^v/me^v (*bottom*) were cultured with M-CSF and 50 ng/ml RANKL (*left*), 50 ng/ml TNFα (*center*), or 20 ng/ml LPS (*right*) for 6 d in the presence or absence of OPG, XT3 (anti-TNFα antagonistic antibody), or control antibody (ACK4) for 6 d. The mean number and SD of $TRAP^+$ MNCs per well from the simultaneous experiments are shown. Significant differences compared with the responses of untreated cultures are indicated by an *asterisk* ($P < 0.05$). In all experiments, no $TRAP^+$ cells were observed without M-CSF.

LPS-responsive OCPs in me^v/me^v BM cells are enriched in the Kit-positive population

It has been reported that OCPs in the BM are enriched in the Kit^+ cell fraction when osteoclastogenesis was induced with stromal cells (40) or with M-CSF and RANKL (41). To assess the phenotypic characterization of LPS-responsive OCPs in BM cells, we enriched the Kit^+ cells using magnetic cell sorting (Fig. 5A) and induced osteoclastogenesis by addition of M-CSF plus RANKL or M-CSF plus LPS. In +/? BM cells, OCPs were enriched in the bound fraction of anti-Kit antibody and magnetic beads. Although a few $TRAP^+$ MNCs were induced from unfractionated +/? BM cells, the Kit^+ cell-enriched fraction gave rise to significant numbers of $TRAP^+$ MNCs in cultures. A few $TRAP^+$ mononuclear cells (data not shown), but few $TRAP^+$ MNCs, were observed in the Kit^- cell fraction (Fig. 5B).

Kit^+ cell-enriched populations from me^v/me^v BM cells contained more cells that expressed high levels of Kit than those from +/? BM cells (Fig. 5A). When the same numbers (2×10^4/well) of Kit^+ cells enriched from me^v/me^v BM cells as +/? BM cells were cultured with M-CSF and RANKL or M-CSF and LPS, the numbers of $TRAP^+$ MNCs in unfractionated and Kit^+ cell-enriched BM cells were comparable, although those from the cell fraction passed through the magnetic bead column were dramatically reduced (Fig. 5B). It is possible that macrophage-like cells overgrew in the wells of the Kit^+ cell-enriched fraction, resulting in saturation of osteoclastogenesis. Because Kit^+ cells proliferated at high levels in the presence of M-CSF, and when 25% of me^v/me^v BM cells were cultured, M-CSF plus RANKL-responding and M-CSF plus LPS-responding OCPs were significantly enriched in the column-bound fraction (Fig. 5B). Therefore, the majority of OCPs in me^v/me^v BM cells might also be present in the Kit^+ cell-enriched fraction.

Moreover, to confirm whether LPS-responsive OCPs express Kit, we precultured BM cells with M-CSF for 3 d and dish-adherent cells were harvested. A majority (+/?; 87.4%, and me^v/me^v; 88.6%) of the precultured cells expressed Mac-1, and half (+/?; 52.2%, and me^v/me^v; 50.2%) of the cells

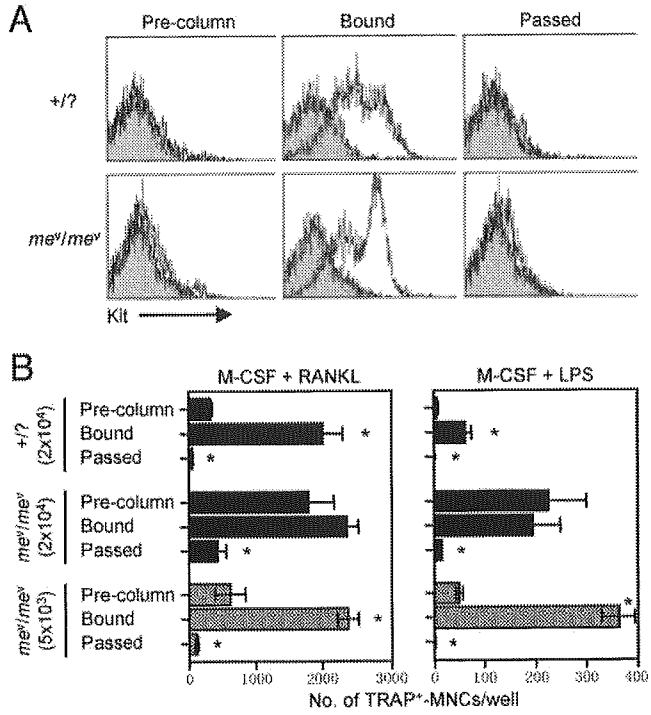

FIG. 5. Osteoclastogenesis from the Kit^+ BM cell-enriched population. The me^v/me^v and +/? littermate BM cells were incubated with PE-labeled anti-Kit antibody (ACK2) and subsequently with anti-PE antibody-conjugated beads (pre-column cells). The cells were applied to the magnetic bead columns, and nonbound cells (passed) and cells bound to the columns (bound) were recovered. A, One aliquot of cells was analyzed by flow cytometry. Cells stained with PE-streptavidin were used as a negative control (*shadowed*). B, Other aliquots of cells (■, 2×10^4/well; ▨, 5×10^3/well) were cultured with 50 ng/ml M-CSF and 50 ng/ml RANKL or with M-CSF and 20 ng/ml LPS. On d 6 of culture, the number of $TRAP^+$ MNCs was counted. Addition of M-CSF alone induced no $TRAP^+$ MNCs or fewer than seven $TRAP^+$ mononuclear cells from either mouse strain.

were also Fms^+; however, few (+/?; 0.32%, and me^v/me^v; 0.12%) of the precultured cells expressed Kit. The harvested cells were further cultured with M-CSF and RANKL, LPS, or RANKL plus LPS for 6 d. In the presence of M-CSF and RANKL, $TRAP^+$ MNCs were generated from both me^v/me^v and +/? precultured BM cells, and me^v/me^v cells gave rise to significantly higher numbers of $TRAP^+$ MNCs than +/? cells (Fig. 6B). In contrast, few of precultured BM cells gave rise to $TRAP^+$ MNCs in the presence of M-CSF and LPS, and addition of LPS inhibited osteoclastogenesis induced by M-CSF and RANKL (Fig. 6, B and C) (29). These results indicate that BM cells precultured with M-CSF lose Kit-expression, and these cells from me^v/me^v mice lose the potential of LPS-responsive differentiation into osteoclasts.

Reduction of osteoclastogenesis from me^v/me^v PECs

Recently, we reported that OCPs in BM and extramedullary organs, such as peritoneal cavity expressed distinct characteristics (29). To assess the influence of SHP-1 deficiency on OCPs in peritoneal cavities, we cultured PECs from me^v/me^v mice and their +/? littermates with M-CSF plus RANKL for 6 d. In the presence of M-CSF and RANKL, the number of $TRAP^+$ MNCs generated from me^v/me^v PECs was signifi-

cantly reduced compared with that from +/? littermates (Fig. 7A). The *me*^{v}/*me*^{v} BM cells cultured in corresponding experiments (experiments 1–3 in Fig. 1A) generated higher numbers of TRAP^{+} MNCs than the wild-type controls. The addition of LPS, TNFα, or IL-1α did not induce osteoclastogenesis in the presence of M-CSF (Fig. 7B). LPS and TNFα inhibited osteoclastogenesis induced by M-CSF and RANKL in control PECs as reported previously (29). IL-1α increased slightly the number of TRAP^{+} MNCs from wild-type PECs by M-CSF and RANKL. In contrast, osteoclast development from *me*^{v}/*me*^{v} PECs was absent or extremely low in all conditions tested (Fig. 7B).

In flow cytometric analysis, Mac-1^{+} cells were 22.6% and 21.9%, and Mac-1^{+} Fms^{+} cells were 12.6% and 9.6% of the cell fraction in +/? and *me*^{v}/*me*^{v} PECs, respectively. Therefore, the contents of the cell lineage in both strains of mice were similar. The *me*^{v}/*me*^{v} PECs may contain cells that inhibited osteoclast maturation, resulting in suppression of osteoclast development from *me*^{v}/*me*^{v} PECs, although cells with the potential to differentiate into mature osteoclasts in the *me*^{v}/*me*^{v} peritoneal cavity may be present. To examine this possibility, we performed mixing experiments with PECs from B6 mice. The number of TRAP^{+} MNCs in mixed cultures was almost additive to that in each PEC from B6 and *me*^{v}/*me*^{v}, and B6 and +/? mice (Fig. 7C). This indicates that *me*^{v}/*me*^{v} PECs may lack OCPs, or the OCPs in *me*^{v}/*me*^{v} PECs may lose differentiative potential, rather than be inhibited by cells in their peritoneal cavity.

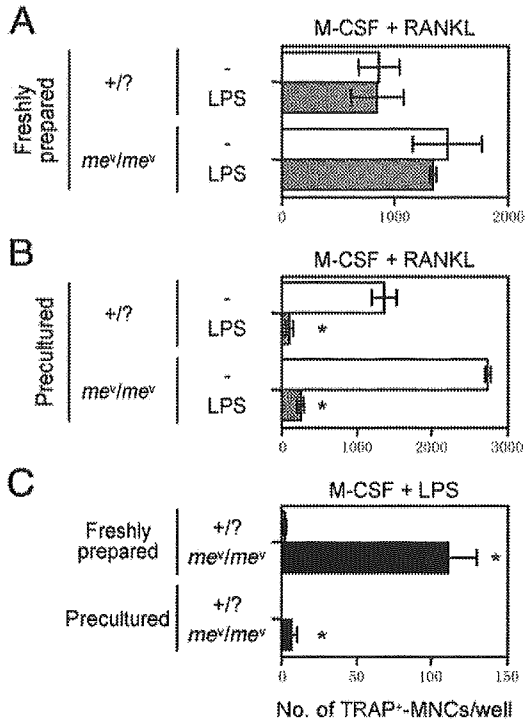

FIG. 6. Few precultured BM cells with M-CSF give rise to osteoclasts in the presence of M-CSF and LPS. A, Freshly prepared BM cells (2×10^4/well) were cultured with (▨) or without (□) LPS in the presence of M-CSF and RANKL for 6 d. B, BM cells (5×10^6/dish) were cultured with 50 ng/ml M-CSF. On d 3, the harvested cells (4×10^3/well) were cultured with (▨) or without (□) LPS in the presence of M-CSF and RANKL for 6 d. C, Freshly prepared (2×10^4/well) or precultured (4×10^3/well) BM cells from *me*^{v}/*me*^{v} mice (■) or +/? littermates (□) were cultured with LPS and M-CSF for 6 d. The number of TRAP^{+} MNCs in a well were counted. Significant differences compared with the responses (B) without LPS or those of +/? littermates (C) are indicated by an *asterisk* ($P < 0.05$).

Discussion

In this study we showed that BM cells from *me*^{v}/*me*^{v} mice defective in SHP-1 gave rise to mature osteoclasts in the presence of M-CSF and LPS without exogenous RANKL or TNFα in culture. It has been reported that the multinucleation and bone resorption of *me*^{v}/*me*^{v} osteoclasts induced by M-CSF and RANKL or by coculturing with stromal cells are accelerated (12, 13). Therefore, the total numbers of TRAP^{+}-cells (mononuclear and multinuclear cells) were relatively comparable, but the numbers of TRAP^{+} MNCs in *me*^{v}/*me*^{v} cultures were significantly higher than those in +/? littermates (12, 13) (Hayashi, S.-I., unpublished observation). Wild-type BM cells gave rise to TRAP^{+} mononuclear cells in the presence of M-CSF and LPS; however, none or only a few multinucleated cells were observed in culture. Moreover, the numbers of TRAP^{+} mononuclear cells in +/? control mice were also significantly lower than those in SHP-1-deficient *me*^{v}/*me*^{v} BM cells.

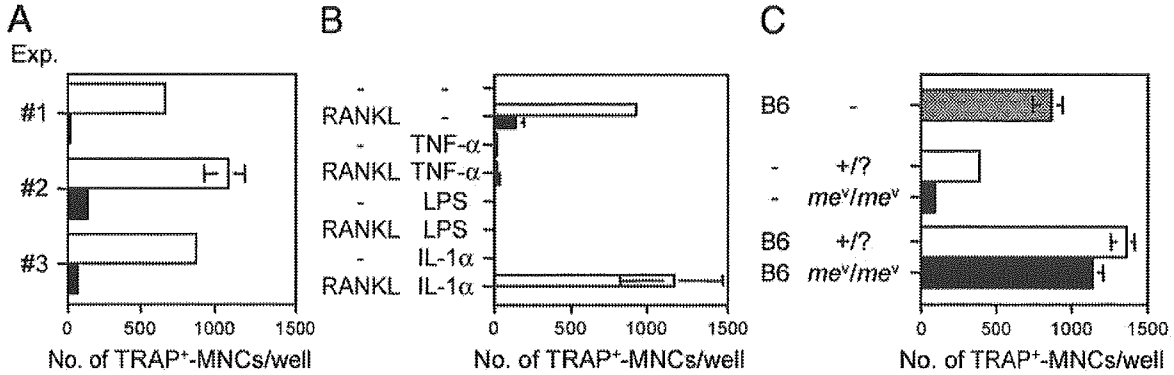

FIG. 7. Osteoclastogenesis from *me*^{v}/*me*^{v} PECs. A, PECs (10×10^4/well) from *me*^{v}/*me*^{v} mice (■) or +/? littermates (□) were cultured with M-CSF and RANKL for 6 d. The number of TRAP^{+} MNCs from three representative experiments in corresponding experiments in Fig. 1A were demonstrated. B, PECs were cultured with RANKL and/or TNFα, LPS, or IL-1α in the presence of M-CSF. C, PECs (5×10^4/well) from B6 mice were cultured without (▨) or with those from *me*^{v}/*me*^{v} (■) or +/? littermates (□) in the presence of M-CSF and RANKL. In all experiments, no TRAP^{+} cells were observed without M-CSF.

Previously, we reported that OCPs in the normal BM were enriched in Kit^+ cells (40, 42). In the current study OCPs in +/? BM responding to M-CSF plus RANKL were enriched in the Kit^+ cell-enriched population. Almost all $TRAP^+$ mononuclear cells induced by M-CSF and LPS were derived from this fraction. OCPs responding to both RANKL and LPS in me^v/me^v BM were also enriched in the magnetic bead column-bound fraction. Kit^+ cell-enriched populations from me^v/me^v BM cells expressed a higher level of Kit per cell than those from +/? cells. Few BM cells precultured with M-CSF for 3 d expressed Kit. In the presence of M-CSF and RANKL, osteoclasts were generated from both me^v/me^v and +/? precultured BM cells. In contrast, precultured BM cells gave rise to few $TRAP^+$ MNCs in the presence of M-CSF and LPS. Moreover, LPS inhibited osteoclastogenesis induced by M-CSF and RANKL (29). Corresponding to losing Kit expression of BM cells precultured with M-CSF, these cells from me^v/me^v mice lose the potential of LPS-responsive differentiation into osteoclasts. These results indicated that the majority of LPS-responsive OCPs as well as RANKL-responsive OCPs in freshly prepared me^v/me^v BM cell populations might be present in the Kit^+ cell fraction (29).

It is noted that a majority of c-Kit^+ cells in freshly prepared BM cells are immature before expressing RANK (41). Lam *et al.* (20) proposed that TNFα could induce osteoclast differentiation only in precursors simultaneously or previously exposed to RANKL. Their conclusion was based on the results that BM cells cultured for 3 d with M-CSF and OPG lost the potential of TNFα-induced osteoclastogenesis, although they also mentioned that overnight preincubation with M-CSF and OPG did not affect their potential of responsiveness to TNFα (20). A majority of OCPs that respond to LPS and differentiate into osteoclasts are Kit^+ cells, which might not express RANK. Even if previous exposure to RANKL is needed to maintain the responsiveness to LPS or TNFα in OCPs, OPG addition from 3 d before or from the initiation of culture must result in the same effect. We confirmed that overnight incubation with M-CSF and OPG did not affect the potential of LPS-induced osteoclastogenesis in me^v/me^v BM cells (data not shown). As Lam *et al.* (20) demonstrated, the presence of RANKL might be optimal for the maintenance of this potential; however, regardless of presence or absence of OPG, 3-d preculture with M-CSF reduced the potential to differentiate into osteoclasts induced by TNFα (29) or LPS. Moreover, several recent studies using RANK-KO mice showed that osteoclastogenesis is induced without RANK/RANKL signaling (18, 19). Therefore, LPS-induced osteoclastogenesis from me^v/me^v BM cells may be independent of RANK/RANKL signaling.

To assess whether me^v/me^v BM contains more Kit^+ cells than +/? BM, flow cytometric analyses were performed repeatedly (data not shown). Some me^v/me^v BM contained a slightly higher ratio of Kit^+ cells than +/? BM, but others were comparable to the wild-type BM. As me^v/me^v Kit^+ cell-enriched populations still generated higher numbers of osteoclasts than Kit^+ cell-enriched +/? populations, the presence of more Kit^+ cells in me^v/me^v BM might not account for the accelerated osteoclastogenesis. Using a limiting dilution assay, we assessed the frequency of OCPs in BM (40). The me^v/me^v mice and +/? littermates contained, on the average, one OCP per 45.3 BM cells and one OCP per 34.8 BM cells, respectively. Single OCPs of me^v/me^v and +/? BM gave rise to 7.1 ± 9.6 and 11.8 ± 21.7 $TRAP^+$ cells, respectively. The frequency of OCPs in BM cells and the growth of OCPs in culture are comparable to those in +/? littermates.

LPS, but not PGN or CpG, induced osteoclastogenesis of me^v/me^v BM cells in the presence of M-CSF. These three TLRs (TLR2, -4, and -9) share the downstream signaling, MyD88, TRAF6, NF-κB, and MAPK, but only TLR4, a receptor for LPS, is known to be another signaling pathway independent of independent of MyD88 (23, 43, 44). LPS might mimic the function of RANKL/RANK signaling, but not that of M-CSF/Fms signaling, in me^v/me^v BM osteoclastogenesis. In the absence of M-CSF, me^v/me^v BM osteoclastogenesis was not observed even if RANKL and LPS were added to the culture (data not shown). SHP-1 is reported to negatively regulate signaling via receptor protein tyrosine kinases, but the ligands, such as stem cell factor, vascular endothelial growth factor 164, platelet-derived growth factor, or insulin could not replace M-CSF function (45) (Yamada, T., unpublished observation). In addition to M-CSF, at least 1 ng/ml RANKL or TNFα is necessary to induce osteoclastogenesis in both me^v/me^v and their littermate (+/?) BM cells. M-CSF plus LPS-induced osteoclastogenesis was not inhibited by either OPG or anti-TNFα Ab. A recent report demonstrated that enriched BM macrophages cultured with M-CSF and thioglycolate-activated peritoneal macrophages produced less than 400 pg/ml TNFα ((28). As we used whole BM cells in the steady state, less than 1/20th of the cell populations and approximately 1/50th of the LPS concentration were comparable to this report, and it is unlikely that our cultures contained more than 1 ng/ml TNFα. Therefore, production of RANKL or TNFα might not be involved in LPS-induced osteoclastogenesis of me^v/me^v BM cells.

Recently, it was shown that RANKL/RANK signaling activates SHP-1 recruitment to the complex containing TRAF6, and SHP-1 blocked the interaction of TRAF6 with the RANK signaling pathway (25). This suggests that SHP-1 might function in the TLR and TRAF6 signaling pathway. Mice lacking either triggering receptor expressed on myeloid cells 2 (TREM2) (46) or DAP12 are reported to develop osteopetrosis (47). These mice have fewer osteoclasts and lack the ability for bone resorption. DAP12, containing a cytoplasmic immunoreceptor tyrosine-based activation motif, is a TREM-related receptor, which recruits SHP-1. The me^v/me^v BM cells accelerate multinucleation (Fig. 1) and bone resorption (12, 13). DAP12 dephosphorylation may be delayed in me^v/me^v BM cells, resulting in an increase in multinucleated osteoclasts.

After addition of PD098059, a MAPK kinase inhibitor, to the culture for 6 d, the total number of $TRAP^+$ cells was relatively comparable to that in the absence of this reagent (data not shown). However, the number of $TRAP^+$ MNCs was significantly reduced. MEK/ERK signaling may be involved in multinucleation of osteoclasts, suggesting that SHP-1 regulates the MEK/ERK signaling pathway. Moreover, as it is known that downstream signaling of TREM and DAP12 activate ERK, SHP-1 deficiency may accelerate ERK activation, resulting in an increase in multinucleated osteoclasts.

Recently, we demonstrated that peritoneal OCPs lose the potential to differentiate into mature osteoclasts if they were exposed to TLR ligands, TNFα, or even RANKL before an encounter with M-CSF and RANKL as a differentiation signal (29). Because SHP-1 deficiency accelerates this signaling pathway, OCPs in the me^v/me^v peritoneal cavity may lose the potential by the exposure of their ligands or unknown natural ligands. Finally, experiments using me^v/me^v mice lacking RANK or RANKL will provide conclusive evidence as to whether LPS may induce osteoclastogenesis *in vivo*. If so, LPS injection should cure the osteopetrosis in the double-mutant mice.

Acknowledgments

We acknowledge Drs. Kensuke Miyake (Tokyo University, Tokyo, Japan), Masato Ogata (Mie University, Mie, Japan), and Nobuyuki Udagawa (Matsumoto Dental University, Nagano, Japan) for helpful suggestions, and Masayuki Takahashi and Takao Taki (Otsuka Pharmaceutical Co. Ltd., Tokushima, Japan) for M-CSF. We also thank Drs. Tomohiro Kurosaki (RIKEN Yokohama Institute, Yokohama, Japan) for his warm encouragement, and Ms. Toshie Shinohara for her secretarial assistance.

Received February 10, 2004. Accepted February 17, 2004.

Address all correspondence and requests for reprints to: Dr. Shin-Ichi Hayashi, Division of Immunology, Department of Molecular and Cellular Biology, School of Life Science, Faculty of Medicine, Tottori University, 86 Nishi-Machi, Yonago, Tottori 683-8503, Japan. E-mail: shayashi@grape.med.tottori-u.ac.jp.

This work was supported by a Grant-in-Aid for Scientific Research (C) from the Ministry of Education, Culture, Sports, Science, and Technology; the Japanese government (to S.I.H. and H.Y.); the Molecular Medical Science Institute, Otsuka Pharmaceutical Co., Ltd.; and NIH Grant CA20408 (to L.D.S.).

Current address for T.Y.: Laboratory for Lymphocyte Differentiation, Research Center for Allergy and Immunology, RIKEN Yokohama Institute, Yokohama 230-0045, Japan.

References

1. **Suda T, Udagawa N, Takahashi N** 1996 Cells of bone: osteoclast generation. In: Bilezikian JP, Raisz LG, Roden GA, eds. Principles of bone biology. New York: Academic Press; 87–102
2. **Hayashi SI, Yamane T, Miyamoto A, Hemmi H, Tagaya H, Tanio Y, Kanda H, Yamazaki H, Kunisada T** 1998 Commitment and differentiation of stem cells to the osteoclast lineage. Biochem Cell Biol 76:911–922
3. **Roodman GD** 1999 Cell biology of the osteoclast. Exp Hematol 27:1229–1241
4. **Theill LE, Boyle WJ, Penninger JM** 2002 RANK-L and RANK: T cells, bone loss, and mammalian evolution. Annu Rev Immunol 20:795–823
5. **Wiktor-Jedrzejczak W, Ahmed A, Szczylik C, Skelly RR** 1982 Hematological characterization of congenital osteopetrosis in *op/op* mouse. J Exp Med 156: 1516–1527
6. **Yoshida H, Hayashi SI, Kunisada T, Ogawa M, Nishikawa S, Okamura H, Sudo T, Shultz LD, Nishikawa S** 1990 The murine mutation osteopetrosis is in the coding region of the macrophage colony stimulating factor gene. Nature 345:442–444
7. **Lagasse E, Weissman IL** 1997 Enforced expression of Bcl-2 in monocytes rescues macrophages and partially reverses osteopetrosis in *op/op* mice. Cell 89:1021–1031
8. **Begg SK, Radley JM, Pollard JW, Chisholm OT, Stanley ER, Bertoncello I** 1993 Delayed hematopoietic development in osteopetrotic (*op/op*) mice. J Exp Med 177:237–242
9. **Niida S, Kaku M, Amano H, Yoshida H, Kataoka H, Nishikawa S, Tanne K, Maeda N, Nishikawa S, Kodama H** 1999 Vascular endothelial growth factor can substitute for macrophage colony-stimulating factor in the support of osteoclastic bone resorption. J Exp Med 190:293–298
10. **Shultz LD, Schweitzer PA, Rajan TV, Yi T, Ihle JN, Matthews RJ, Thomas ML, Beier DR** 1993 Mutations at the murine motheaten locus are within the hematopoietic cell protein-tyrosine phosphatase (*Hcph*) gene. Cell 73:1445–1454
11. **Shultz LD, Rajan TV, Greiner DL** 1997 Severe defects in immunity and hematopoiesis caused by SHP-1 protein-tyrosine-phosphatase deficiency. Trends Biotechnol 15:302–307
12. **Umeda S, Beamer WG, Takagi K, Naito M, Hayashi SI, Yonemitsu H, Yi T, Shultz LD** 1999 Deficiency of SHP-1 protein-tyrosine phosphatase activity results in heightened osteoclast function and decreased bone density. Am J Pathol 155:223–233
13. **Aoki K, Didomenico E, Sims NA, Mukhopadhyay K, Neff L, Houghton A, Amling M, Levy JB, Horne WC, Baron R** 1999 The tyrosine phosphatase SHP-1 is a negative regulator of osteoclastogenesis and osteoclast resorbing activity: increased resorption and osteopenia in me^v/me^v mutant mice. Bone 25:261–267
14. **Yasuda H, Shima N, Nakagawa N, Yamaguchi K, Kinosaki M, Mochizuki S, Tomoyasu A, Yano K, Goto M, Murakami A, Tsuda E, Morinaga T, Higashio K, Udagawa N, Takahashi N, Suda T** 1998 Osteoclast differentiation factor is a ligand for osteoprotegerin/osteoclastogenesis-inhibitory factor and is identical to TRANCE/RANKL. Proc Natl Acad Sci USA 95:3597–3602
15. **Lacey DL, Timms E, Tan HL, Kelley MJ, Dunstan CR, Burgess T, Elliott R, Colombero A, Elliott G, Scully S, Hsu H, Sullivan J, Hawkins N, Davy E, Capparelli C, Eli A, Qian YX, Kaufman S, Sarosi I, Shalhoub V, Senaldi G, Guo J, Delaney J, Boyle WJ** 1998 Osteoprotegerin ligand is a cytokine that regulates osteoclast differentiation and activation. Cell 93:165–176
16. **Kong YY, Yoshida H, Sarosi I, Tan HL, Timms E, Capparelli C, Morony S, Oliveira-dos-Santos AJ, Van G, Itie A, Khoo W, Wakeham A, Dunstan CR, Lacey DL, Mak TW, Boyle WJ, Penninger JM** 1999 OPGL is a key regulator of osteoclastogenesis, lymphocyte development and lymph-node organogenesis. Nature 397:315–323
17. **Dougall WC, Glaccum M, Charrier K, Rohrbach K, Brasel K, De Smedt T, Daro E, Smith J, Tometsko ME, Maliszewski CR, Armstrong A, Shen V, Bain S, Cosman D, Anderson D, Morrissey PJ, Peschon JJ, Schuh J** 1999 RANK is essential for osteoclast and lymph node development. Genes Dev 13:2412–2424
18. **Li J, Sarosi I, Yan XQ, Morony S, Capparelli C, Tan HL, McCabe S, Elliott R, Scully S, Van G, Kaufman S, Juan SC, Sun Y, Tarpley J, Martin L, Christensen K, McCabe J, Kostenuik P, Hsu H, Fletcher F, Dunstan CR, Lacey DL, Boyle WJ** 2000 RANK is the intrinsic hematopoietic cell surface receptor that controls osteoclastogenesis and regulation of bone mass and calcium metabolism. Proc Natl Acad Sci USA 97:1566–1571
19. **Yamashita T, Xing L, Li P, Schwarz EM, Dougall WC, Boyce F** 2002 C-Fos over-expression induces osteoclastogenesis independent of RANK signaling. J Bone Miner Res 17(Suppl 1):S131
20. **Lam J, Takeshita S, Barker JE, Kanagawa O, Ross FP, Teitelbaum SL** 2000 TNF-α induces osteoclastogenesis by directed stimulation of macrophages exposed to permissive levels of RANK ligand. J Clin Invest 106:1481–1488
21. **Kobayashi K, Takahashi N, Jimi E, Udagawa N, Takami M, Kotake S, Nakagawa N, Kinosaki M, Yamaguchi K, Shima N, Yasuda H, Morinaga T, Higashio K, Martin TJ, Suda T** 2000 Tumor necrosis factor α stimulates osteoclast differentiation by a mechanism independent of the ODF/RANKL-RANK interaction. J Exp Med 191:275–286
22. **Naito A, Azuma S, Tanaka S, Miyazaki T, Takaki S, Takatsu K, Nakao K, Nakamura K, Katsuki M, Yamamoto T, Inoue J** 1999 Severe osteopetrosis, defective interleukin-1 signalling and lymph node organogenesis in TRAF6-deficient mice. Genes Cells 4:353–362
23. **Akira S, Takeda K, Kaisho T** 2001 Toll-like receptors: critical proteins linking innate and acquired immunity. Nat Immunol 2:675–680
24. **Janeway Jr CA, Medzhitov R** 2002 Innate immune recognition. Annu Rev Immunol 20:197–216
25. **Zhang Z, Jimi E, Bothwell AL** 2003 Receptor activator of NF-κB ligand stimulates recruitment of SHP-1 to the complex containing TNFR-associated factor 6 that regulates osteoclastogenesis. J Immunol 171:3620–3626
26. **Takayanagi H, Ogasawara K, Hida S, Chiba T, Murata S, Sato K, Takaoka A, Yokochi T, Oda H, Tanaka K, Nakamura K, Taniguchi T** 2000 T-cell-mediated regulation of osteoclastogenesis by signalling cross-talk between RANKL and IFN-γ. Nature 408:600–605
27. **Takami M, Kim N, Rho J, Choi Y** 2002 Stimulation by Toll-like receptors inhibits osteoclast differentiation. J Immunol 169:1516–1523
28. **Itoh K, Udagawa N, Kobayashi K, Suda K, Li X, Takami M, Okahashi N, Nishihara T, Takahashi N** 2003 Lipopolysaccharide promotes the survival of osteoclasts via Toll-like receptor 4, but cytokine production of osteoclasts in response to lipopolysaccharide is different from that of macrophages. J Immunol 170:3688–3695
29. **Hayashi SI, Yamada T, Tsuneto M, Yamane T, Takahashi M, Shultz LD, Yamazaki H** 2003 Distinct osteoclast precursors in the bone marrow and extramedullary organs characterized by responsiveness to Toll-like receptor ligands and TNF-α. J Immunol 171:5130–5139
30. **Yamada T, Yamazaki H, Yamane T, Yoshino M, Okuyama H, Tsuneto M, Kurino T, Hayashi SI, Sakano S** 2003 Regulation of osteoclast development by Notch signaling directed to osteoclast precursors and through stromal cells. Blood 101:2227–2234
31. **Miyamoto A, Kunisada T, Hemmi H, Yamane T, Yasuda H, Miyake K, Yamazaki H, Hayashi SI** 1998 Establishment and characterization of an immortal macrophage-like cell line inducible to differentiate to osteoclasts. Biochem Biophys Res Commun 242:703–709
32. **Shevde N, Anklesaria P, Greenberger JS, Bleiberg I, Glowacki J** 1994 Stromal cell-mediated stimulation of osteoclastogenesis. Proc Soc Exp Biol Med 205: 306–315
33. **Hemmi H, Takeuchi O, Kawai T, Kaisho T, Sato S, Sanjo H, Matsumoto M,**

Hoshino K, Wagner H, Takeda K, Akira S 2000 A Toll-like receptor recognizes bacterial DNA. Nature 408:740–745
34. **Ogawa M, Matsuzaki Y, Nishikawa S, Hayashi SI, Kunisada T, Sudo T, Kina T, Nakauchi H, Nishikawa S** 1991 Expression and function of c-kit in hemopoietic progenitor cells. J Exp Med 174:63–71
35. **Sudo T, Nishikawa S, Ogawa M, Kataoka H, Ohno N, Izawa A, Hayashi SI, Nishikawa S** 1995 Functional hierarchy of c-kit and c-fms in intramarrow production of CFU-M. Oncogene 11:2469–2476
36. **Poltorak A, He X, Smirnova I, Liu MY, Van Huffel C, Du X, Birdwell D, Alejos E, Silva M, Galanos C, Freudenberg M, Ricciardi-Castagnoli P, Layton B, Beutler B** 1998 Defective LPS signaling in C3H/HeJ and C57BL/10ScCr mice: mutations in Tlr4 gene. Science 282:2085–2088
37. **Aliprantis AO, Yang RB, Mark MR, Suggett S, Devaux B, Radolf JD, Klimpel GR, Godowski P, Zychlinsky A** 1999 Cell activation and apoptosis by bacterial lipoproteins through Toll-like receptor-2. Science 285:736–739
38. **Zou W, Schwartz H, Endres S, Hartmann G, Bar-Shavit Z** 2002 CpG oligonucleotides: novel regulators of osteoclast differentiation. FASEB J 16:274–282
39. **Kobayashi K, Hernandez LD, Galan JE, Janeway Jr CA, Medzhitov R, Flavell RA** 2002 IRAK-M is a negative regulator of Toll-like receptor signaling. Cell 110:191–202
40. **Hayashi SI, Miyamoto A, Yamane T, Kataoka H, Ogawa M, Sugawara S, Nishikawa S, Nishikawa S, Sudo T, Yamazaki H, Kunisada T** 1997 Osteoclast precursors in bone marrow and peritoneal cavity. J Cell Physiol 170:241–247
41. **Arai F, Miyamoto T, Ohneda O, Inada T, Sudo T, Brasel K, Miyata T, Anderson DM, Suda T** 1999 Commitment and differentiation of osteoclast precursor cells by the sequential expression of c-Fms and receptor activator of nuclear factor κB (RANK) receptors. J Exp Med 190:1741–1754
42. **Yamazaki H, Kunisada T, Yamane T, Hayashi SI** 2001 Presence of osteoclast precursors in the colonies cloned in the presence of hematopoietic colony-stimulating factors. Exp Hematol 29:68–76
43. **Nomura F, Akashi S, Sakao Y, Sato S, Kawai T, Matsumoto M, Nakanishi K, Kimoto M, Miyake K, Takeda K, Akira S** 2000 Endotoxin tolerance in mouse peritoneal macrophages correlates with down-regulation of surface toll-like receptor 4 expression. J Immunol 164:3476–3479
44. **Castrillo A, Sean B. Joseph SB, Vaidya SA, Haberland M, Fogelman AM, Cheng G, Tontonoz P** 2003 Crosstalk between LXR and Toll-like receptor signaling mediates bacterial and viral antagonism of cholesterol metabolism. Mol Cell 12:805–816
45. **Okuyama H, Tsuneto M, Yamane T, Yamazaki H, Hayashi, SI** 2003 Discrete types of osteoclast precursors can be generated from embryonic stem cells. Stem Cells 21:670–680
46. **Colonna M** 2003 TREMs in the immune system and beyond. Nat Rev Immunol 3:445–453
47. **Kaifu T, Nakahara J, Inui M, Mishima K, Momiyama T, Kaji M, Sugahara A, Koito H, Ujike-Asai A, Nakamura A, Kanazawa K, Tan-Takeuchi K, Iwasaki K, Yokoyama WM, Kudo A, Fujiwara M, Asou H, Takai T** 2003 Osteopetrosis and thalamic hypomyelinosis with synaptic degeneration in DAP12-deficient mice. J Clin Invest 111:323–332

Endocrinology **is published monthly by The Endocrine Society (http://www.endo-society.org), the foremost professional society serving the endocrine community.**

ELSEVIER

Bone 35 (2004) 1120–1126

BONE

www.elsevier.com/locate/bone

Detection of osteoclastic cell–cell fusion through retroviral vector packaging

Takako Kondo[a], Kyoji Ikeda[a], Koichi Matsuo[a,b,*]

[a]*Department of Geriatric Research, National Institute for Longevity Sciences (NILS), Aichi 474-8522, Japan*
[b]*Department of Microbiology and Immunology, School of Medicine, Keio University, Tokyo 160-8582, Japan*

Received 30 April 2004; revised 14 June 2004; accepted 17 June 2004
Available online 9 September 2004

Abstract

Cell–cell fusion generates multinucleated cells such as osteoclasts in bone, myotubes in muscle, and trophoblasts in placenta. Molecular details governing these fusion processes are still largely unknown. As a step toward identification of fusogenic genes, we tested the concept that retroviral vectors can be packaged as a result of cell–cell fusion. First, we introduced replication-deficient retroviral vectors expressing mCAT-1, which mediates fusogenic interaction with the retroviral envelope protein Env, into Chinese hamster ovary (CHO) cells to generate vector cells. Plasmids expressing virion proteins Gag, Pol, and Env were introduced into a separate culture of CHO cells to generate packaging cells. Co-culturing vector and packaging cells resulted in production of infectious retroviruses carrying the mCAT-1 gene as a consequence of cell–cell fusion. Second, we introduced a retroviral vector into primary osteoclast precursors and co-cultured them with established osteoclast precursor RAW264.7 cells, which turned out to harbor packaging activity. Packaged retroviral vector was detected in culture supernatants only where the osteoclast differentiation factor receptor activator for NF-κB ligand (RANKL) induced fusion between these two cell types. These data suggest that retrovirus production can occur as a result of cell–cell fusion. This provides a novel approach for isolating and characterizing fusogenic genes using retroviral expression vectors.

Keywords: Retrovirus; Fusion; Osteoclasts

Introduction

Osteoclasts are cells that resorb bone [1]. Mononuclear osteoclast precursors of the monocyte-macrophage lineage fuse with each other in the presence of stromal factors such as macrophage-colony stimulating factor (M-CSF, also known as CSF-1) and receptor activator for NF-κB ligand (RANKL). The resulting multinucleated osteoclasts may contain from 3 to more than 20 nuclei. Macrophages also have the potential to form multinucleated cells called giant cells or polykarions at sites of chronic inflammation.

Various fusogenic molecules induce cell–cell fusion during mammalian development [2]. The gamete fusion process requires a disintegrin and metalloproteinase 2, fertilin β (ADAM 2) on the sperm [3], and integrin α6β1 and CD9 on the egg [4,5]. Multinucleated myotube formation involves a fertilin-related molecule, ADAM12 (meltrin α) [6], and other molecules [7]. Candidate molecules involved in fusion of osteoclasts or macrophages include ADAMs, especially ADAM9 [8], the purinergic $P2X_7$ receptor [9], terminal high mannose type oligosaccharide-mannose receptor [10], E-cadherin [11], CD98 (also known as fusion regulatory protein-1) [12], CD44, macrophage fusion receptor (MFR, also known as P84/SHPS-1/SIRP/BIT), and the ligand CD47 [13,14]. On the contrary, tetraspanin proteins CD9 and CD81 prevent the fusion of mononuclear phagocytes [15]. Most of these nonviral fusogenic and anti-fusion molecules have been character-

* Corresponding author. Department of Microbiology and Immunology, School of Medicine, Keio University, 35 Shinanomachi, Shinjuku-ku, Tokyo 160-8582, Japan. Fax: +81 3 5360 1508.
E-mail address: matsuo@sc.itc.keio.ac.jp (K. Matsuo).

8756-3282/$ - see front matter © 2004 Elsevier Inc. All rights reserved.
doi:10.1016/j.bone.2004.06.011

ized by loss-of-function experiments where cell–cell fusion is blocked either by antibodies or soluble recombinant extracellular domains. Identification and analysis of fusogenic molecules in gain-of-function experiments should give further insights into fusion mechanisms in the osteoclast-macrophage lineage.

Enveloped viruses such as retrovirus and influenza virus express glycoproteins that induce fusion of viral and cellular membranes to initiate infection [16]. The envelope glycoprotein Env of Moloney murine leukemia viruses (MLV) is fusogenic and induces virus–cell fusion by interacting with the mouse ecotropic receptor mCAT-1, a cationic amino-acid transporter [17–19]. This interaction between Env and mCAT-1 can also induce cell–cell fusion. MLV usually does not infect CHO cells because CHO cells do not express receptors for MLV. However, when mCAT-1 is overexpressed in CHO cells, these cells become susceptible to MLV and form abundant syncytia in the presence of the viruses [20].

As an initial step to identify and analyze fusogenic genes by gain-of-function experiments, we developed model systems to demonstrate that retroviruses can be produced as a result of cell–cell fusion. Commonly used retroviral vectors lack coding capacity for viral proteins and thus cannot replicate as viruses once gene-transfer is completed. These vectors are usually prepared as plasmids and transfected into packaging cell lines, which provide retroviral proteins Gag (for group-specific antigens), Pol, and Env, and release infectious viral particles into the culture supernatant. In our system, retroviral genomes were introduced into packaging cells via cell–cell fusion. We observed infectious retroviral production as a consequence of cell–cell fusion, establishing the basis for a novel strategy to characterize osteoclast fusion mechanisms.

Materials and methods

Retroviral vectors and cells

The retroviral vectors pBabe puro [21] and pFB neo (Stratagene) express inserted genes from the MLV long terminal repeat (LTR). pBabe puro-GFP and pFB neo-GFP were generated by inserting the 0.7-kb *Bam*HI–*Eco*RI fragment of phrGFP-1 (Stratagene) into pBabe puro and pFB neo, respectively. pFB neo-mCAT1-GFP was constructed by inserting the 2.7-kb *Bam*HI–*Not*I fragment of pmCAT1-GFP [22] into pFB neo. CHO cells were cultured in Dulbecco's modified Eagle's medium supplemented with 10% fetal calf serum (FCS). CHOpac was generated by sequential lipofection and antibiotic selection of CHO cells with pEnv-IRES-puro [23] in 5 μg/ml puromycin, and pGag-pol-IRES-bsr [23] in 3 μg/ml blasticidin, so that the expression of viral structural proteins Gag, Pol, and Env was driven by the *EF1*α promoter. CHOgfp and CHOmcat were generated by lipofection of CHO cells with pFB neo-GFP and pFB neo-mCAT1-GFP, respectively, followed by selection in 500 μg/ml G418. RAW264.7 cells [24] (ATCC TIB-71) were cultured in α-minimum essential medium (MEM) supplemented with 10% FCS. RAWpac cells were generated by sequential lipofection and selection of RAW264.7 cells with pEnv-IRES-puro in 5 μg/ml puromycin and pGag-pol-IRES-bsr in 1 μg/ml blasticidin. M-CSF-dependent murine bone marrow-derived macrophages were prepared from C57BL/6 mice as described [25] and maintained in α-MEM supplemented with 10% FCS and 30 ng/ml M-CSF (R&D). Mvec cells were generated by infecting these primary macrophages with pBabe puro-GFP or pFB neo-GFP viruses produced using Plat-E packaging cells [23]. Cell–cell fusion of RAW264.7 and Mvec cells was induced by adding 25 ng/ml recombinant mouse RANKL (R&D) to the culture medium. For titration of viruses, Rat-1A fibroblasts (ATCC JHU-25) were plated at 5000 cells/48 well, infected with serially diluted culture supernatants, and selected in 2.5 μg/ml puromycin or 500 μg/ml G418, and colonies were stained with 0.2% methylene blue in methanol.

Gene reporter-based cell fusion assay

p5G-luc-SV/Zeo was constructed by inserting a 150-bp *Sac*I–*Pvu*II fragment of 5G-OVEC containing five times multimerized binding sites for GAL4 [26] and an *Xho*I–*Bam*HI fragment containing the zeocin resistance gene of pSV40/Zeo2 (Invitrogen) into *Sac*I–*Pvu*II and *Bam*HI–*Sal*I of pGL3-Basic vector (Promega), respectively. pcDNA3.1/Zeo(+)-GAL4-VP16 was constructed by inserting a PCR-amplified coding region of GAL4(1–93)-VP16(413–490) [26] into pcDNA3.1/Zeo (Invitrogen) such that expression would be driven by the cytomegalovirus promoter. CHOpac+gluc was generated by transfecting p5G-luc-SV/Zeo into CHOpac cells and selecting under 400 μg/ml zeocin, 5 μg/ml puromycin, and 3 μg/ml blasticidin. CHOmcat+vp16 was generated by transfecting pcDNA3.1/Zeo(+)-Gal4-VP16 into CHOmcat cells and selecting under 400 μg/ml zeocin and 500 μg/ml G418. To monitor cell–cell fusion, cells were plated at 2000 cells/48 well and harvested in lysis buffer at 6, 12, and 24 h after the start of co-culture. Luciferase activity was measured using the dual-luciferase reporter assay system (Promega).

Other methods

Northern blotting was performed with *IRES*, *gag-pol*, and *env* probes, which were the 1-kb *Not*I–*Sal*I fragment of pGag-pol-IRES-bsr, the 2.1-kb *Sal*I–*Not*I fragment of pGag-pol-IRES-bsr, and the 2-kb *Eco*RI–*Not*I fragment of pEnv-IRES-puro, respectively. Southern blotting was performed using *Sal*I-digested genomic DNA of infected Rat-1A cells and a 765-bp hrGFP probe. Tartrate-resistant acid phosphatase (TRAP) staining was performed with the leukocyte acid phosphatase kit (SIGMA) after fixing in

3.7% formaldehyde for 30 min and in acetone/ethanol (50:50) for 30 s. Immunofluorescence microscopy was performed to identify F-actin microfilament. Briefly, cells were fixed in 4% paraformaldehyde for 10 min, washed twice with PBS for 5 min each, treated with 0.1% Triton X-100 in PBS for 10 min, stained with 5 U/ml phalloidin-conjugated rhodamine (Molecular Probes) for 45 min, washed twice for 5 min each, and mounted with DAPI to stain nuclei.

Results

Experimental design

To examine whether retroviral particles can be produced as a result of cell–cell fusion, we developed a novel strategy that requires "vector cells" and "packaging cells" (Fig. 1). The vector cells carry an integrated retroviral vector containing an intact packaging signal (ψ) and an antibiotic resistant gene (R) but no retroviral proteins, while the packaging cells express retroviral proteins, Gag, Pol, and Env. We examined whether production of infectious retroviruses occurs when these two types of cells fuse with each other. In the following experiments, cell–cell fusion was induced in two different ways: by expressing a fusion-inducing gene (F) from the retroviral vector or by adding the osteoclastogenic cytokine RANKL to the culture media of osteoclast precursors.

Fusion of CHO cells

We chose the ecotropic receptor mCAT-1 as a model fusion-inducing gene based on the observation that over-expression of mCAT-1 in CHO cells not only makes CHO cells susceptible to MLV infection, but also induces

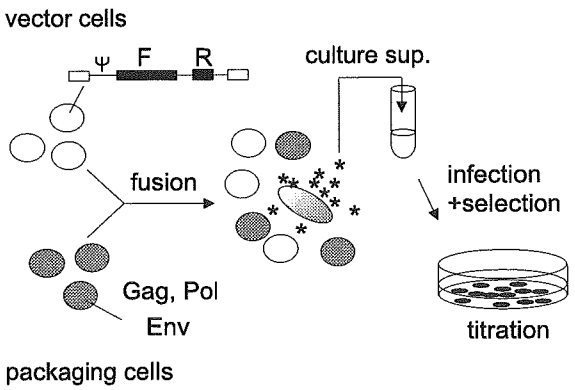

Fig. 1. Experimental design for detecting retroviral production upon cell–cell fusion. Vector cells (white) carry integrated proviral DNAs, and packaging cells (gray) express viral proteins, Gag, Pol, and Env. Fusion of these two cell types results in release of infectious retroviral particles into culture supernatant. F: a fusion-inducing gene (mCAT-1-GFP) or a green fluorescent protein (GFP) gene. R: puromycin- or G418-resistance gene. These genes are used to select cells infected with culture supernatants.

syncytia formation through the interaction between mCAT-1 and the fusogenic viral glycoprotein Env [20]. We generated vector cells by introducing pFB neo-mCAT1-GFP into CHO cells so that the resulting CHOmcat cells expressed the receptor mCAT-1 fused to GFP [22]. CHO cells carrying pFB neo-GFP (CHOgfp) served as a negative control. We then generated CHOpac by introducing expression vectors for Gag, Pol, and Env into CHO cells. CHOmcat, CHOgfp, and parental CHO cells were cultured alone or co-cultured with CHOpac. These cells were morphologically indistinguishable and do not fuse spontaneously (data not shown). As expected, fused cells were observed under the microscope when CHOmcat cells were co-cultured with CHOpac (Fig. 2). The multinucleated cells were GFP-positive, indicating that they expressed mCAT-1-GFP protein. To demonstrate that these cells were not aggregated cells and that cell–cell fusion was occurring between CHOmcat and CHOpac cells, we devised a gene reporter-based cell fusion assay. This assay makes use of the synthetic transcription factor GAL4-VP16 containing a DNA-binding domain of the yeast transcription factor GAL4 linked to a transactivation domain of the herpes simplex virus transcription factor VP16. As a reporter, we used the luciferase gene driven by a promoter containing GAL4 binding sites. We expressed GAL4-VP16 in CHOpac and the luciferase reporter in CHOmcat cells. As shown in Fig. 3, luciferase activity was significantly elevated 24 h after co-culturing CHOmcat and CHOpac cells, suggesting that fusion had occurred between these two types of cells. We tested for the presence of infectious retroviral vectors pFB neo-mCAT1-GFP in culture supernatants by infection of Rat-1A fibroblasts followed by G418 selection. Significant numbers of G418-resistant and GFP-positive Rat-1A cell colonies were observed when the co-culture supernatants of CHOmcat and CHOpac were titrated (175 $\pm$ 35 cfu/ml). Such colonies were not observed with supernatants of CHO, CHOgfp, CHOmcat, or CHOpac cells alone, or co-cultures of all combinations of the two cell populations other than CHOmcat and CHOpac. These data show that cell–cell fusion can result in the production of infectious retroviruses carrying a fusion-inducing gene.

RAW264.7 cells harbor endogenous packaging activity

The murine macrophage cell line RAW264.7 was originally established from a tumor induced by Abelson-murine leukemia virus (A-MLV) [24]. These cells form multinucleated osteoclast-like cells via cell–cell fusion in response to RANKL and are extensively used in the study of osteoclast biology. Although RAW264.7 cells do not produce infectious retroviruses by themselves [24], we unexpectedly detected infectious retroviruses in the culture supernatant after transfecting the retroviral vector pBabe puro-GFP into RAW264.7 cells. The titer measured in fibroblasts was 2500 and 770 cfu/ml for transient and stable transfection, respectively. Control NIH3T3 fibroblasts pro-

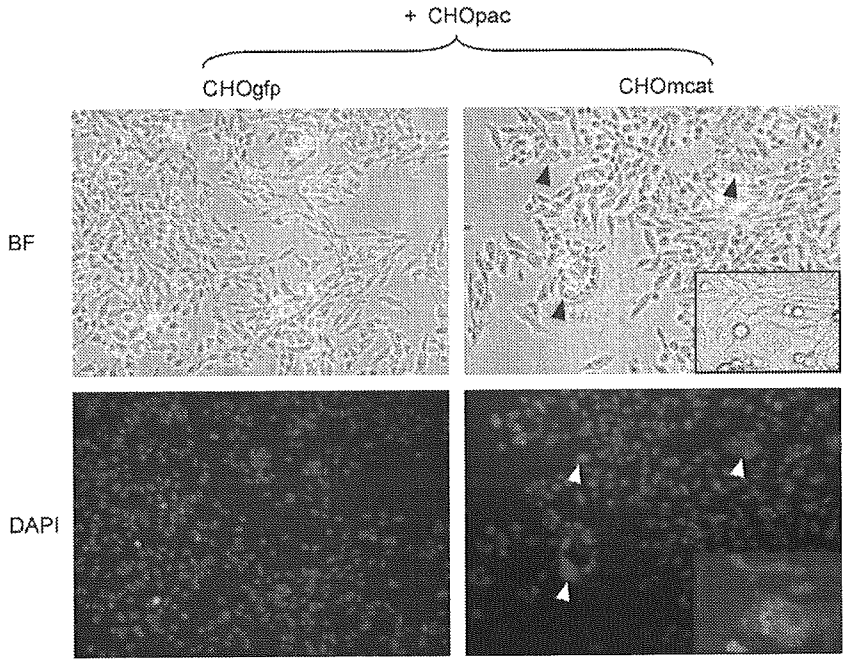

Fig. 2. Fusion of CHO-derived cells. CHOgft or CHOmcat was co-cultured with CHOpac cells. Bright field (BF) and DAPI staining of nuclei are shown. Arrowheads indicate multinucleated cells. The insets show that multinucleated cells in bright field are GFP-positive under fluorescence.

duced no infectious retrovirus upon transfection, as expected (data not shown). In an attempt to boost packaging activity of RAW264.7 cells, we stably introduced two plasmids that were originally used to establish the Plat-E conventional packaging cell line [23] expressing Gag, Pol, and Env into RAW264.7 cells. Three independent subclones of RAW264.7, designated RAWpac cells, were obtained, but the viral titers of their supernatants (2700 cfu/ml for transient transfection) were not significantly higher than that of parental RAW264.7 cells. Consistent with the observation that RAW264.7 cells could package retroviruses, Northern blot analysis showed that RNA from parental RAW264.7 cells hybridized with *gag-pol* and *env* probes (Fig. 4). These transcripts were not observed in other murine cell lines, such as NIH3T3 fibroblasts and Ba/F3 pro-B cells. Therefore, we concluded that the parental RAW264.7 cells harbor packaging activity and used these cells as packaging cells in the following experiments.

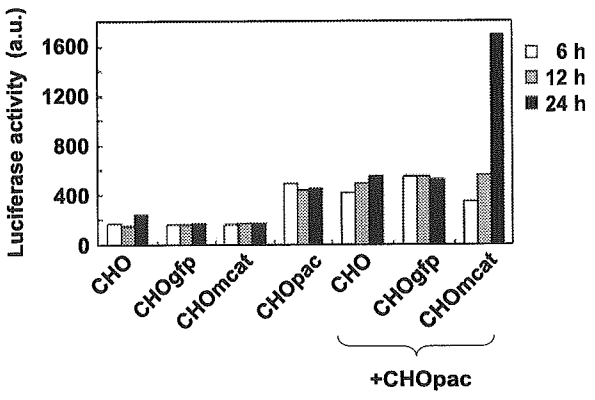

Fig. 3. Gene reporter-based cell fusion assay. A GAL4-VP16 transcription factor was expressed in CHOmcat (CHOmcat + vp16) cells and a GAL4-dependent luciferase reporter gene was introduced into CHOpac (CHOpac + gluc) cells. Cell lysates were prepared at the indicated times after the start of co-culture. a.u., arbitrary units.

Fusion-induced packaging of retroviral vectors

Because RAW264.7 cells have an intrinsic packaging activity, they are not suitable to generate vector cells, which should carry defective retroviral vectors without any viral production. Therefore, we prepared primary bone marrow

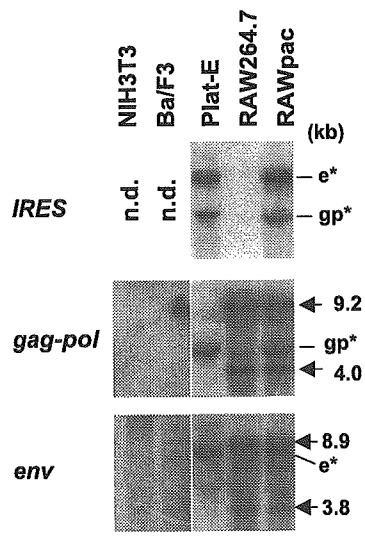

Fig. 4. RAW264.7 cells express endogenous *gag-pol* and *env* transcripts. Estimated sizes of endogenous transcripts are indicated. Exogenous *gag-pol* (gp*) and *env* (e*) transcripts were detected with the *IRES* probe. Plat-E is a packaging cell line.

macrophages and infected them with pBabe puro-GFP virus to generate vector cells, which we designated Mvec. Either Mvec or RAW264.7 cells alone, or 50:50 mixture of Mvec and RAW264.7 cells was cultured in the absence or presence of RANKL (Fig. 5). On day 4, the culture supernatants were harvested and the viral titer was determined using Rat-1A fibroblasts. Either Mvec or RAW264.7 cells alone formed multinucleated cells dependent on RANKL (Figs. 5D, E, G, and H). Infection experiments using the supernatant from Mvec or RAW264.7 cells did not produce puromycin-resistant fibroblast colonies regardless of cell–cell fusion events. When Mvec and RAW264.7 cells were co-cultured, many irregularly shaped multinucleated cells were formed (Figs. 5F and I). These multinucleated cells were likely a result of fusion events between Mvec and RAW264.7 cells. The co-culture supernatant of Mvec and RAW264.7 cells in the presence of RANKL produced puromycin-resistant colonies that were GFP-positive. No such colonies were obtained using supernatant of Mvec or RAW264.7 cells alone, or in the absence of RANKL (Fig. 5). These observations suggest that infectious retroviruses were produced as a consequence of cell–cell fusion between Mvec and RAW264.7 cells. We repeated the experiment by replacing pBabe puro-GFP with another retroviral vector pFB neo-GFP. G418-resistant Rat-1A fibroblast colonies were obtained only when supernatant from co-culture in the presence of RANKL was used. Southern blotting showed that genomic DNA prepared from these G418-resistant colonies contained retroviral DNA, indicating the successful transfer of retroviral vector to fibroblasts (data not shown). These observations demonstrate that cell–cell fusion during osteoclast differentiation can result in retrovirus production.

Discussion

Cells of multicellular organisms, in principle, do not usually fuse with each other. Osteoclasts, however, possess abilities to fuse efficiently with each other during differentiation. Multinucleated osteoclasts seem to provide an advantage in resorption, because the area of the resorption pit surface is linearly correlated to the number of nuclei per osteoclast [27]. We described here model systems demonstrating that cell–cell fusion results in retrovirus production when one cell contains defective retroviral vector and the other produces proteins for retroviral packaging.

In the first model, cell–cell fusion is triggered by interaction between Env expressed on CHOpac cells and the receptor mCAT-1 on CHOmcat cells [20]: CHOpac produced Env as well as Gag and Pol, and a specialized vector cell, CHOmcat, carried a retroviral vector expressing mCAT-1-GFP. Fusion between CHOpac and CHOmcat was detected by a novel cell fusion assay. A luciferase gene driven by a GAL4-dependent promoter was introduced into CHOpac and a chimeric GAL4-VP16 transcription factor

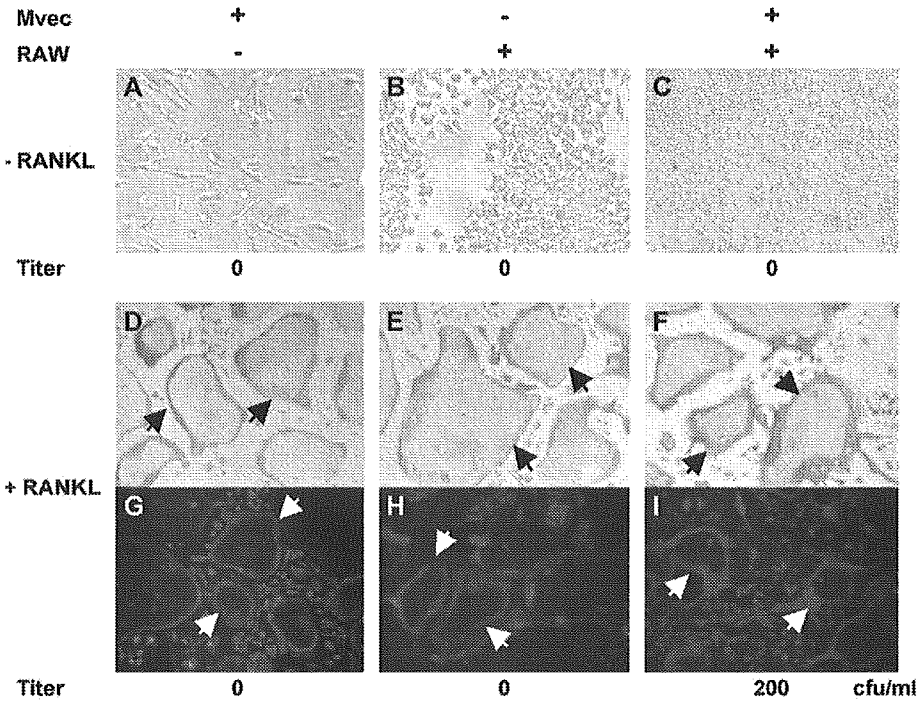

Fig. 5. Production of retroviruses upon osteoclast fusion. Mvec and RAW264.7 (RAW) cells were cultured separately or together (2×10^4/24 well) in the absence or presence of 25 ng/ml RANKL for 3 days. A–C, bright field. D–F, stained for TRAP activity (red). G–I, phalloidin staining for actin (red) and DAPI staining for nuclei (blue). Arrowheads indicate multinucleated osteoclast-like cells. Titer of pBabe puro-GFP virus (cfu/ml) was measured using Rat-1A fibroblasts.

was introduced into CHOmcat. Fusion of these two types of cells provided the reporter gene with the transcription activator and was measured as luciferase activity. Similar complementation-based fusion assays were previously reported using T7 promoter-luciferase construct in one cell and T7 polymerase in the other [28], and an enzymatic *lacZ* complementation [29]. Infectious retroviruses were specifically demonstrated in the supernatant from the fusion-induced co-culture of CHOpac and CHOmcat. The relatively low titer observed suggests that a rescued retroviral vector does not efficiently spread among vec cells, presumably due to competition with "empty" virions produced by pac cells. It is also possible that membrane fusion mediated by mCAT-1 in CHO cells was inefficient due to limited mCAT-1 expression levels [20]. Therefore, cloned CHOmcat sublines expressing mCAT-1 at high levels might result in more efficient cell–cell fusion and higher viral titer than the bulk population of CHOmcat cells used in the experiment.

In the second model, we used the osteoclastogenic cytokine RANKL to induce fusion of RAW264.7 cells with primary macrophages. We observed packaging activity in RAW264.7 cells, which was unexpected because these cells carry a defective A-MLV, and thus do not produce virus [24]. In hindsight, the packaging activity of RAW264.7 cells is consistent with the observations that RAW264.7 cells are highly resistant to retroviral gene transfer, unlike primary osteoclast precursors, which are susceptible to retroviral vectors [30,31]. It is conceivable that Env proteins expressed in RAW264.7 cells may fully occupy the receptor mCAT-1. At the mRNA level, RAW264.7 cells express mCAT-1 as abundantly as NIH3T3 cells, and additional introduction of a mCAT-1 expression vector did not improve susceptibility of RAW264.7 cells to murine retroviral infection (our unpublished data). Furthermore, Northern blot experiments showed that *gag-pol* and *env* sequences were transcribed in RAW264.7 cells, and a "signal sequence trap" experiment, which detects signal sequences in cDNA fragments [32], revealed *env* cDNA sequences in RAW264.7 cells (K. Mizuno and K. Watanabe, personal communication). These observations are consistent with the notion that RAW264.7 cells can produce principal retroviral proteins. It should be noted that the use of retroviral vectors in RAW264.7 cells requires extra caution because infectious retroviruses may be produced in culture supernatants. We conclude that the retroviral production is a consequence of cell–cell fusion between Mvec and RAW264.7 cells induced by RANKL. Although unlikely, there may be other explanations. RANKL treatment might induce RAW264.7 cells to produce endogenous retroviruses, which then infect Mvec cells to rescue retroviral vector production. Transwell culture methods separating RAW264.7 cells from Mvec cells should allow us to examine this possibility. Alternatively, Gag, Pol, and Env proteins might be transferred from RAW264.7 cells to Mvec cells without cell–cell fusion, as in the case of retroviral protein Tat or the herpes simplex virus structural protein VP22 [33–35]. However, considering the production of infectious retroviruses in the CHO model, we believe that fusion of osteoclasts is the cause of retroviral production.

Collectively, these observations suggest that retroviral packaging rescue can occur upon cell–cell fusion. Cell–cell fusion can be induced by the cDNA carried by a retroviral vector as in the mCAT-1 model. Therefore, fusion potentials of various putative fusogenic genes and their mutants can be monitored by the release of retroviruses. Furthermore, this provides a new strategy for screening fusogenic genes inserted in retroviral cDNA expression libraries. The cDNA library is constructed in "vector cells" and the fusogenic cDNA can be isolated in infectious retroviruses, which are released via fusion-induced retroviral packaging. With conventional expression vectors, it may be difficult to recover cDNA from a few fused cells because multinucleated cells usually do not proliferate. However, retroviral rescue allows us to amplify cDNA by further infecting proliferating cells. One might think that Env expressed on the surface of "packaging cells" would disturb the natural cell–cell fusion process. However, Env expression does not induce fusion in NIH3T3 cells, which express mCAT-1 abundantly. Therefore, retroviral packaging rescue seems to be applicable to define additional host cell factors facilitating fusion processes. These factors should include both fusion molecules and their positive regulators.

In conclusion, retroviral packaging rescue as described here is a novel approach for producing retroviruses as a consequence of cell–cell fusion and may allow expression cloning and functional analysis of genes responsible for osteoclastic cell–cell fusion.

Acknowledgments

We thank T. Kitamura for pGag-pol-IRES-bsr and pEnv-IRES-puro, M. Masuda for pmCAT1-GFP, H. Hara for CHO cells, and K. Mizuno and K. Watanabe for unpublished sequence information. We thank J. Silver, S. Kato, K. Segawa, N. Ray, and C. Zhao for critical reading of the manuscript. We also thank M. Suzuki for technical support. This work was supported by the Program for Promotion of Fundamental Studies in Health Sciences of the Organization for Pharmaceutical Safety and Research of Japan to K.I.

References

[1] Teitelbaum SL, Ross FP. Genetic regulation of osteoclast development and function. Nat Rev, Genet 2003;4:638–49.
[2] Hernandez LD, Hoffman LR, Wolfsberg TG, White JM. Virus–cell and cell–cell fusion. Annu Rev Cell Dev Biol 1996;12:627–61.
[3] Cho C, Bunch DO, Faure JE, Goulding EH, Eddy EM, Primakoff P, et al. Fertilization defects in sperm from mice lacking fertilin β. Science 1998;281:1857–9.

[4] Almeida EA, Huovila AP, Sutherland AE, Stephens LE, Calarco PG, Shaw LM, et al. Mouse egg integrin α6 β1 functions as a sperm receptor. Cell 1995;81:1095–104.
[5] Kaji K, Oda S, Shikano T, Ohnuki T, Uematsu Y, Sakagami J, et al. The gamete fusion process is defective in eggs of Cd9-deficient mice. Nat Genet 2000;24:279–82.
[6] Yagami-Hiromasa T, Sato T, Kurisaki T, Kamijo K, Nabeshima Y, Fujisawa-Sehara A. A metalloprotease-disintegrin participating in myoblast fusion. Nature 1995;377:652–6.
[7] Horsley V, Pavlath GK. Forming a multinucleated cell: molecules that regulate myoblast fusion. Cells Tissues Organs 2004;176:67–78.
[8] Namba K, Nishio M, Mori K, Miyamoto N, Tsurudome M, Ito M, et al. Involvement of ADAM9 in multinucleated giant cell formation of blood monocytes. Cell Immunol 2001;213:104–13.
[9] Falzoni S, Chiozzi P, Ferrari D, Buell G, Di Virgilio F. P2X(7) receptor and polykarion formation. Mol Biol Cell 2000;11:3169–76.
[10] Morishima S, Morita I, Tokushima T, Kawashima H, Miyasaka M, Omura K, et al. Expression and role of mannose receptor/terminal high-mannose type oligosaccharide on osteoclast precursors during osteoclast formation. J Endocrinol 2003;176:285–92.
[11] Mbalaviele G, Chen H, Boyce BF, Mundy GR, Yoneda T. The role of cadherin in the generation of multinucleated osteoclasts from mononuclear precursors in murine marrow. J Clin Invest 1995;95: 2757–65.
[12] Tajima M, Higuchi S, Higuchi Y, Miyamoto N, Uchida A, Ito M, et al. Suppression of FRP-1/CD98-mediated multinucleated giant cell and osteoclast formation by an anti-FRP-1/CD98 mAb, HBJ 127, that inhibits c-src expression. Cell Immunol 1999;193:162–9.
[13] Saginario C, Sterling H, Beckers C, Kobayashi R, Solimena M, Ullu E, et al. MFR, a putative receptor mediating the fusion of macrophages. Mol Cell Biol 1998;18:6213–23.
[14] Vignery A. Osteoclasts and giant cells: macrophage-macrophage fusion mechanism. Int J Exp Pathol 2000;81:291–304.
[15] Takeda Y, Tachibana I, Miyado K, Kobayashi M, Miyazaki T, Funakoshi T, et al. Tetraspanins CD9 and CD81 function to prevent the fusion of mononuclear phagocytes. J Cell Biol 2003; 161:945–56.
[16] Weissenhorn W, Dessen A, Calder LJ, Harrison SC, Skehel JJ, Wiley DC. Structural basis for membrane fusion by enveloped viruses. Mol Membr Biol 1999;16:3–9.
[17] Kim JW, Closs EI, Albritton LM, Cunningham JM. Transport of cationic amino acids by the mouse ecotropic retrovirus receptor. Nature 1991;352:725–8.
[18] Wang H, Kavanaugh MP, North RA, Kabat D. Cell-surface receptor for ecotropic murine retroviruses is a basic amino-acid transporter. Nature 1991;352:729–31.
[19] Lu X, Xiong Y, Silver J. Asymmetric requirement for cholesterol in receptor-bearing but not envelope-bearing membranes for fusion mediated by ecotropic murine leukemia virus. J Virol 2002;76: 6701–9.
[20] Siess DC, Kozak SL, Kabat D. Exceptional fusogenicity of Chinese hamster ovary cells with murine retroviruses suggests roles for cellular factor(s) and receptor clusters in the membrane fusion process. J Virol 1996;70:3432–9.
[21] Morgenstern JP, Land H. Advanced mammalian gene transfer: high titre retroviral vectors with multiple drug selection markers and a complementary helper-free packaging cell line. Nucleic Acids Res 1990;18:3587–96.
[22] Masuda M, Kakushima N, Wilt SG, Ruscetti SK, Hoffman PM, Iwamoto A. Analysis of receptor usage by ecotropic murine retroviruses, using green fluorescent protein-tagged cationic amino acid transporters. J Virol 1999;73:8623–9.
[23] Morita S, Kojima T, Kitamura T. Plat-E: an efficient and stable system for transient packaging of retroviruses. Gene Ther 2000;7:1063–6.
[24] Raschke WC, Baird S, Ralph P, Nakoinz I. Functional macrophage cell lines transformed by Abelson leukemia virus. Cell 1978;15: 261–7.
[25] Takeshita S, Kaji K, Kudo A. Identification and characterization of the new osteoclast progenitor with macrophage phenotypes being able to differentiate into mature osteoclasts. J Bone Miner Res 2000;15: 1477–8.
[26] Seipel K, Georgiev O, Schaffner W. Different activation domains stimulate transcription from remote ('enhancer') and proximal ('promoter') positions. EMBO J 1992;11:4961–8.
[27] Boissy P, Saltel F, Bouniol C, Jurdic P, Machuca-Gayet I. Transcriptional activity of nuclei in multinucleated osteoclasts and its modulation by calcitonin. Endocrinology 2002;143:1913–21.
[28] Nussbaum O, Broder CC, Berger EA. Fusogenic mechanisms of enveloped-virus glycoproteins analyzed by a novel recombinant vaccinia virus-based assay quantitating cell fusion-dependent reporter gene activation. J Virol 1994;68:5411–22.
[29] Mohler WA, Blau HM. Gene expression and cell fusion analyzed by *lacZ* complementation in mammalian cells. Proc Natl Acad Sci U S A 1996;93:12423–7.
[30] Matsuo K, Owens JM, Tonko M, Elliott C, Chambers TJ, Wagner EF. *Fosl1* is a transcriptional target of c-Fos during osteoclast differentiation. Nat Genet 2000;24:184–7.
[31] Matsuo K, Galson DL, Zhao C, Peng L, Laplace C, Wang KZ, et al. Nuclear factor of activated T-cells (NFAT) rescues osteoclastogenesis in precursors lacking c-Fos. J Biol Chem 2004;279:26475–80.
[32] Kojima T, Kitamura T. A signal sequence trap based on a constitutively active cytokine receptor. Nat Biotechnol 1999;17: 487–90.
[33] Green EA, Flavell RA. TRANCE-RANK, a new signal pathway involved in lymphocyte development and T cell activation. J Exp Med 1999;189:1017–20.
[34] Frankel AD, Pabo CO. Cellular uptake of the tat protein from human immunodeficiency virus. Cell 1988;55:1189–93.
[35] Elliott G, O'Hare P. Intercellular trafficking and protein delivery by a herpesvirus structural protein. Cell 1997;88:223–33.

MEDICAL TOPICS 第14回

γ-グルタミルトランスペプチダーゼ（γ-GTP/GGT）の骨吸収亢進作用

(*Osteoclast forming activity of γ-Glutamyl transpeptidase*)

国立長寿医療センター研究所運動器疾患研究部骨代謝制御研究室室長　**新飯田俊平**　*Shumpei Niida*

Key words：γ-GTP，破骨細胞，骨吸収

はじめに

肝機能マーカーであるγ-GTPは広く市井に行き渡った検査用語の1つである。酒呑みのオジサンたちはその数値に一喜一憂しながらも呑んでいる。むろんγ-Glutamyl transpeptidase[1]のことである。国際標準で表記するならGGTとなるが，ご多分にもれず国際標準など通用しない。わが国ではγ-GTPはこれからもγ-GTPなのだろうが，ここではGGTと表記する。GGTは，一般検査においてはアルカリフォスファターゼ(ALP)などとともに「胆道系酵素」として黄疸の鑑別，肝・胆道系疾患の診断や経過観察に用いられている。GGTは肝細胞の毛細胆管の膜表面に発現し，胆汁うっ滞，アルコール性肝障害，薬剤性肝障害が起こると膜から離れ血中に入るのでその数値が高くなるからである。つまり，血中GGTは主に肝臓由来ということになる。だから肝機能マーカーなのであろう。ある種の癌では発現が高く，その種の腫瘍マーカーになることもある。この酵素が最も大量に発現している臓器は腎臓（近位尿細管）である。GGTは細胞外においてグルタチオンなどのγ-Glutamyl基をほかのタンパクに転移するという重要な役割を担っている。この過程の中にはグルタチオンの分解に依存する細胞内へのシステイン補充という役割が組み込まれている[2]。だから，GGTの欠損が起こるとシステイン欠乏になる。GGT遺伝子欠損マウスでは白内障，短寿命などの老化現象的な症状がみられる[3]。これはGGTによる細胞内へのシステインの供給が途絶え強力な抗酸化物質であるグルタチオンの産生システムが働かず，酸化ストレスに対する恒常性維持機構が破綻したためと考えられている。骨の代謝も不調になり骨粗鬆症様を呈する[4]。これらの症状はシステインの投与で回復するのだから酵素活性に関連した現象と思われる。ところが，本稿で紹介するGGTの作用はこうした酵素活性とは無関係のようである。

骨吸収因子GGTの単離

体の骨は吸収と形成を繰り返している。これを骨のリモデリングという。3年もあればすべての骨は新しくなるらしい。吸収を担当している破骨細胞はマクロファージ系の多核巨細胞である。その証拠に，この細胞の分化にはマクロファージと同じ成長因子(CSF-1/M-CSF)が必須である[5]。CSF-1で誘導された破骨細胞前駆細胞は，骨芽細胞から分泌される破骨細胞分化因子(RANKL/TRELANCE/POGL)によって最終分化を遂げる[6]。CSF-1とRANKLの産生はインターロイキン(IL)-1，IL-6，IL-17，プロスタグランジンE_2，ビタミンD_3などの刺激で上昇する[7]。ほとんどが炎症性の因子だが，骨の分野ではこれらを骨吸収因子と呼ぶ。骨吸収因子は女性ホルモンの欠乏，

リウマチや歯周炎などの炎症で発現が亢進する。

癌や炎症組織からはさまざまなサイトカイン，化学物質が産生される。骨に発生した癌や炎症組織にはまだまだ未知の骨吸収因子の発現があるのではないか。マウスで骨に転移すると顕著な骨破壊を惹起するTリンパ腫細胞(BW5147細胞)の発現遺伝子群を調べてみた。これらの細胞を増殖させて細胞からRNAを取り出す。それらを長さ別にいくつかに分けてアフリカツメガエルの卵の中に入れて培養する。培養液には卵で合成されたTリンパ腫細胞由来のタンパクも分泌されている。それを骨髄細胞の培養に入れてやる。ある長さのRNAフラクションを注入した卵の培養液に強い破骨細胞誘導活性が示されたので，そこからcDNAライブラリーを構築し，再びcRNAにして卵に入れ，同じことを繰り返す(**図1**)。書くと簡単であるが実は大変な作業である。このフラクションからのクローンだけでも63万個もできた。こうした作業を繰り返し，破骨細胞形成活性をもつ遺伝子を絞り込む。単離したものを順にその塩基配列を調べるのだが，すべてが既知のものならこの仕事はそれでおしまいである。ところが，運よく既知の骨吸収因子のリストにないものが含まれていた。

▶ GGTの破骨細胞形成能 ◀

塩基配列のデーターベース検索でGGTがヒットしたときは何かの間違いだと思った。GGT自体は未知のものどころか，酔っ払いのオジサンだって知っている。しかし，骨吸収因子としては新規のものである。GGTに骨吸収活性などあるはずがない。ほとんどの人はそう思うらしい。そこで，ラットの腎臓から精製したGGT(阪大・谷口直之教授提供)を骨髄培養に直接加えてみた。既知の強力な骨吸収因子ほどではないが，この系でも確かに多核の破骨細胞様細胞の誘導が確認された(**図2**)。これらの細胞を象牙板の上で培養すると象牙質を吸収することも確かめた。さらに，

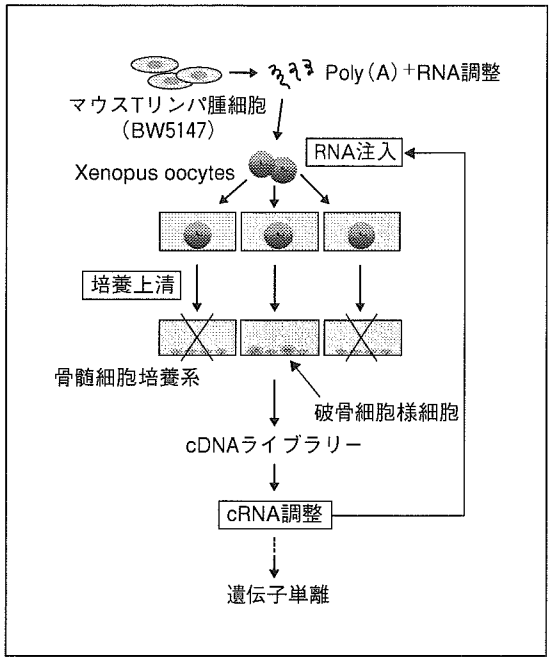

図1．発現クローニング法の略図
マウスTリンパ腫細胞から取り出したRNAをアフリカツメガエル卵に注入してTリンパ腫細胞由来のタンパク合成を代替させる方法で破骨細胞誘導因子を取り出した。

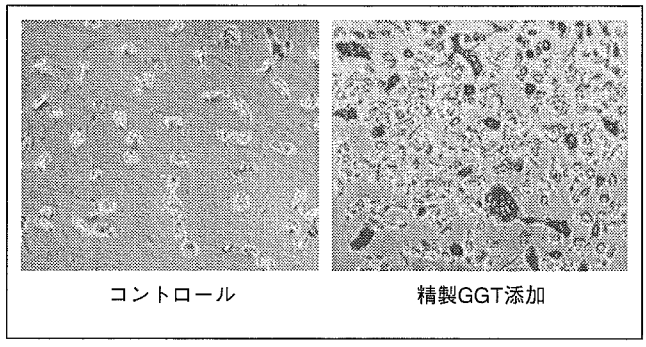

図2．骨髄培養系に精製GGTを添加して誘導された破骨細胞
色の濃い大型の細胞が破骨細胞。

ヒトGGTを遺伝子組換え技術で精製し，再度実験してみたが，結果は同じであった。

次に，GGTを加えた骨髄培養に抗GGT抗体(阪大・谷口教授提供)を入れ，その影響について調べてみた。当然といえば当然であるが，破骨細胞形成と骨吸収活性は抑制された。ところが，この抗体は酵素活性を阻害しない。すなわち，酵素活性があるのに破骨細胞形成活性は消失した。このことはGGTの破骨細胞形成能は，われわれが知るところのGGTの酵素活性とは無関係であることを意味している(**図3**)[8]。そこで，アシビシンという酵素活性阻害物質をGGTに修飾させた不活性型のGGTを精製し，それを骨髄培養に加えてみた。**図4**に示したように，不活性型GGT もまた濃度依存的に破骨細胞形成を誘導することが示された。GGTには酵素活性とは別に，破骨細胞形成能という独立した機能をもつことが明らかになった[8]。

GGTは骨髄培養においてRANKLの発現を誘導する

骨吸収因子の多くは最終分化因子であるRANKLの発現誘導因子である。RANKLは骨芽細胞から分泌される膜結合型のタンパクであるが，骨芽細胞の発現する各骨吸収因子の受容体を介してその発現が誘導される。そこで，GGTがRANKLを誘導しているのかどうか調べてみた。RANKLの囮受容体であるオステオプロテジェリン(OPG)という破骨細胞分化抑制タンパクがある[9]。これは生体内でも働いているもので，破骨細胞の分化を負に調節している。このタンパクの欠損マウスはたちまち骨粗鬆症になる[10]。負の調節が働かなくなったので骨吸収が暴走した結果である。このタンパクをGGTで誘導される破骨細胞の系に入れると濃度依存的に細胞数は減少した。すなわち，GGTによる破骨細胞形成はRANKLに依存していると考えられる。実際，GGTで刺激された骨髄培養系ではRANKLのmRNAの発現上昇がみられる(**図5**)。加えて，タンパクレベルの上昇も確認され[8]，GGTはRANKL発現を誘導するタイプの骨吸収因子であ

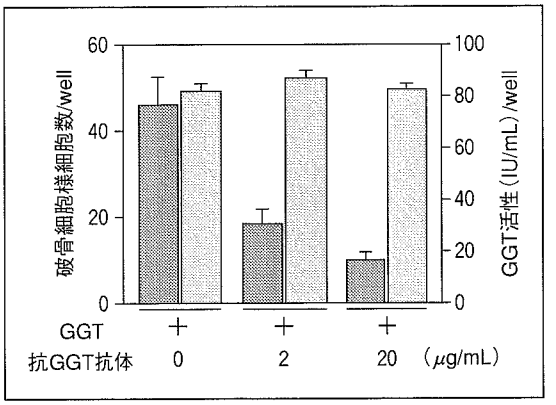

図3．GGTの破骨細胞形成能と酵素活性
GGTによる破骨細胞形成は抗GGT抗体によって用量依存的に抑制されたが，酵素活性は中和されていない。
(文献8より引用・改変)

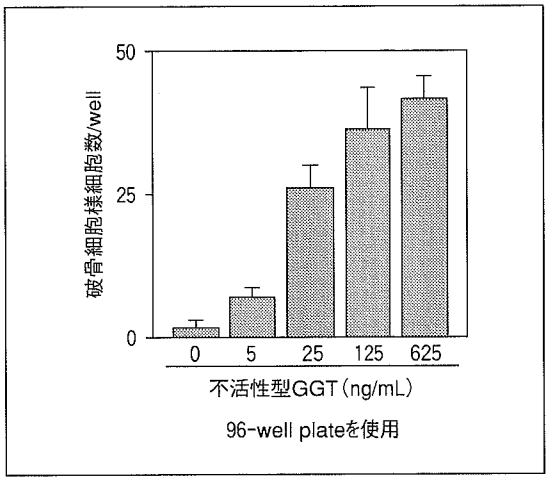

図4．不活性型GGTによる破骨細胞形成
GGTの酵素活性を化学的に不活性化したGGTを作製して骨髄培養系に添加しても，破骨細胞の形成が起こる。
(文献8より引用・改変)

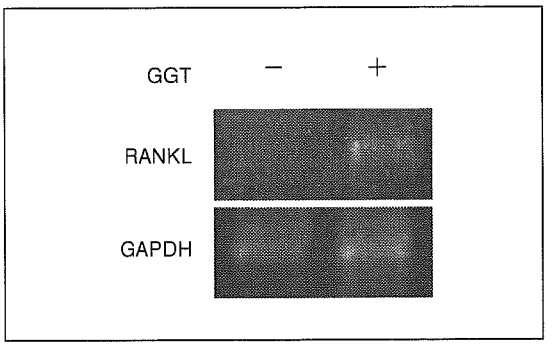

図5．GGTを添加した骨髄培養における破骨細胞分化因子RANKLの発現亢進
(文献8より引用・改変)

ることが示された。

繰り返しになるが，GGTの破骨細胞誘導には酵素活性は関係ない。それならどのようにしてRANKL発現を誘導するのか。それぞれの骨吸収因子は骨芽細胞の膜表面にある特定の受容体に結合して細胞内にRANKL発現のためのシグナルを送る。それならGGTにも受容体があるのではないか。GGTが骨吸収因子かもしれないというのだから，その受容体があるくらい不思議なことではない。

▶ GGTは病的な骨吸収因子 ◀

GGTは実際にはどういうところで骨吸収因子として働いているのか。GGTは先にも述べたように腎臓や肝臓で発現している。そのほか，膵臓や腸上皮，唾液腺などの管腔上皮で発現しているが，およそ骨とは縁がなさそうである。しかし，骨にできたある種の癌だけでなく，関節炎などの炎症でもGGT発現が亢進することがわかってきた。これらについては現在調べている最中で，詳細について記載することができず残念であるが，今のところ病的な環境下で発現する局所的骨破壊因子ではないか，と考えている。

それなら，血中GGT値が高いと骨粗鬆症になるのか。そういう疑問が生じる。骨粗鬆症患者はGGTが高い，という話は聞いたことがない。私たちの研究部ではGGTを過剰発現するトランスジェニックマウスを作製し，その解析を進めている。このマウスの血中GGTは正常マウスの何倍もある。骨量も正常マウスより低下していることがわかった。GGTの過剰発現は確かに骨代謝に影響するようだ。マウスの話だが，GGTは欠損しても過剰になっても骨粗鬆症の要因になるらしい。いずれにしてもその詳細は今後の研究を待つしかない。ヒトの例を探してみると，アルコール依存症の人は高い血中GGT濃度を維持している。こういう人たちの骨量は減少傾向を示すことが知られている[11]。これはアルコールで骨形成の方が抑制されるからだといわれているが，今回のことからGGTが骨吸収側に働いている可能性もあるのではないか。脂肪肝の人でも血中GGTが高いことがある。しかし，骨量が減っているかどうは知らない。誰か調べられたら是非結果を知らせてほしい。

▶ おわりに ◀

古い検査値の解説書には，「GGTはALPと異なり骨疾患で上昇しない」と注釈しているものもある。これはALPが成長期の骨で強く発現しているので検査値を読むときに注意が必要であることに対比させた，いわば「配慮」であったと思われる。その配慮も近頃ではみることがない。おそらく配慮が不要なくらい常識化したからであろう。しかし，今回の研究はその常識に異論を唱える結果となった。ひょっとすると，今度は「常識」を見直すための「配慮」が必要になるかもしれない。

謝　辞

GGTをクローニングした石塚保行博士(株式会社エーシーバイオテクノロジーズ，国立長寿医療センター研究所外来研究員)，多大なご協力をいただいた谷口直之教授(阪大医学部)，池田義孝講師(現・佐賀大医学部教授)をはじめこの研究に参加していただいた共同研究者各位に心から感謝いたします。

文　献

1) Protein reviews on the web : http : //www.ncbi. nih. gov/PROW/guide/1398792298_g. htm
2) Taniguchi N, Ikeda Y : γ-Glutamyl transpeptidase ; catalytic mechanism and gene expression. Adv Enzymol Relat Areas Mol Biol **72** : 239-278, 1998
3) Lieberman MW, Wiseman AL, Shi ZZ, et al : Growth retardation and cysteine deficiency in γ-glutamyl transpeptidase-deficient mice. Proc Natl Acad Sci U S A **93** : 7923-7926, 1996
4) Levasseur R, Barrios R, Elefteriou F, et al : Reversible skeletal abnormalities in γ-glutamyl transpeptidase-deficient mice. Endocrinology **144** : 2761-2764, 2003
5) Yoshida H, Hayashi S, Kunisada T, et al : The murine mutation osteopetrosis is in the coding region of the macrophage colony stimulating factor gene. Nature **345** : 442-444, 1990

6) Yasuda H, Shima N, Nakagawa N, et al : Osteoclast differentiation factor is a ligand for osteoprotegerin/osteoclastogenesis-inhibitory factor and is identical to TRANCE/RANKL. Proc Natl Acad Sci U S A **95** : 3597-3602, 1998
7) Suda T, Takahashi N, Udagawa N, et al : Modulation of osteoclast differentiation and function by the new members of the tumor necrosis factor receptor and ligand families. Endocr Rev **20** : 345-357, 1999
8) Niida S, Kawahara M, Ishizuka Y, et al : γ-Glutamyltraspeptidase stimulates RANKL expression independent of its enzymatic activity and serves as a pathological bone-resorbing factor. J Biol Chem **279** : 5752-5756, 2004
9) Yasuda H, Shima N, Nakagawa N, et al : Identity of osteoclastogenesis inhibitory factor (OCIF) and osteoprotegerin (OPG) ; a mechanism by which OPG/OCIF inhibits osteoclastogenesis *in vitro*. Endocrinology **139** : 1329-1337, 1998
10) Bucay N, Sarosi I, Dunstan CR, et al : osteoprotegerin-deficient mice develop early onset osteoporosis and arterial calcification. Genes Dev **12** : 1260-1268, 1998
11) Santolaria F, Gonzalez-Reimers E, Perez-Manzano JL, et al : Osteopenia assessed by body composition analysis is related to malnutrition in alcoholic patients. Alcohol **22** : 147-157, 2000